Response to

Request for Additional Information No. 82
(1082, 1096, 1107, 1113, 1125, 1151, 1098, 1097), Supplement 3

10/03/2008

U. S. EPR Standard Design Certification
AREVA NP Inc.
Docket No. 52-020
SRP Section: 06.02.01 - Containment Functional Design
SRP Section: 06.02.01.02 - Subcompartment Analysis
SRP Section: 06.02.01.03 - Mass and Energy Release Analysis for Postulated Loss-of-Coolant Accidents (LOCAs)
SRP Section: 06.02.01.04 - Mass and Energy Release Analysis for Postulated Secondary System Pipe Ruptures
SRP Section: 06.02.01.05 - Minimum Containment Pressure Analysis for Emergency Core Cooling System Performance Capability Studies
SRP Section: 06.02.02 - Containment Heat Removal Systems
SRP Section: 06.02.04 - Containment Isolation System
SRP Section: 06.02.06 - Containment Leakage Testing
Application Section: FSAR Ch. 6
SPCV Branch

Question 06.02.01-12:

RAI 6.2.1.1-1

a. Steam Line Break Calculations (FSAR Section 6.2.1.1.3)

1. Only one power level (50%) was investigated in the large span between 20% initial power level and 80% initial power level. This analysis at 50% initial power level produced the limiting temperature and pressure for the design of the U.S. EPR containment. Perhaps the peak containment pressure and temperature lie at an intermediate power level. Provide additional analysis for double ended main steam line breaks at intermediate power levels so that the power level producing the most severe containment results may be identified.

2. Section 6.2.1.4.1.3 states that emergency feedwater flow to the affected steam generator is assumed to be terminated 30 minutes (1800 seconds) after the break by the plant operators. Figures 6.2.1-34 and 6.2.1-35 provide containment pressure and temperature analyses for only 500 seconds. Since there are no active safety systems to provide containment atmospheric cooling at EPR, extend the containment analysis until steam flow from the postulated main steam line break is terminated.

3. For the spectrum of main steam line breaks analyzed, the calculated containment vapor temperature for some cases exceeded the specified containment design temperature of 338°F. Explain why exceeding the design temperature is acceptable. Provide appropriate COL interface requirements (COL Information Item) for instrumentation within the containment so that adequately qualified equipment may be installed.

b. Negative Containment Pressure Analysis (FSAR Section 6.2.1.1.1)

1. Section 6.2.1.1.1 lists 5 potential events which cause negative pressure across the containment wall. So that the staff may perform a review, provide a complete description of the calculation which was performed in each case including the assumptions and justification that the assumptions and methodology are conservative for containment analysis. For example for the post accident cooldown scenario, the leakage of air from the containment before isolation should be evaluated and the details of the evaluation should be described in the response.

2. A sudden containment temperature reduction is said to produce the largest negative pressure of 2.92 psi which is said to be within the external design of the building. Provide the maximum negative differential pressure that would be within the structural design of the reactor building and provide reference to the FSAR section where the structural design is described.

c. Containment Atmospheric Mixing and Heat Transfer Modeling (FSAR Section 6.2.1.1.3)

1. Describe and justify the heat transfer correlations that are used with the GOTHIC containment building model to describe heat transfer to the containment heat structures following a LOCA. For both LOCA and MSLB calculations describe and

justify the differences in assumptions for heat transfer coefficients between vertical and horizontal surfaces within containment.

2. Provide an analysis of IRWST pool stratification following a large break LOCA and include the following information.

   i. Justify that the assumptions made for pool surface temperature in calculations of atmospheric heat transfer to the pool are conservative.

   ii. FSAR Figures 3.8.2 and 6.3-5 appear to show a vertical partition bisecting the IRWST. The IRWST drawings in ANP-10293 do not appear to show such a partition. Describe the function of the partition and its effect on IRWST mixing.

   iii. FSAR Figures 3.8-11, 3.8.12 and 3.8.13 seem to show that the section of ceiling over the IRWST which is under the pressurizer is about 3 feet lower than the rest of the IRWST ceiling. Discuss the effect of the lowered ceiling area on heat transfer to the IRWST surface in particular for raised post-accident IRWST water levels.

3. The Containment Building is separated into a central portion containing the reactor system and a peripheral lower temperature portion containing equipment. Separation is accomplished by compartment walls, foils, doors, and dampers. The foils are located above the steam generator compartments and are designed to open at a fraction of a psi. The doors and dampers located at lower elevations and must also open to avoid stratification so that steam flowing to the containment dome can circulate down the containment walls to reach the heat structures an the containment lower elevations. The doors and dampers are designed to open at various pressures from a few psi to greater than 13 psi. The staff is concerned that the foils above the reactor system will open and cause pressure to be equalized throughout the containment building. With the pressure equalized the doors and dampers needed to promote circulation and prevent stratification may not open. Provide justification that sufficient compartment dampers and doors will open and to discuss impact on containment circulation if only a portion of the dampers and doors are open following a LOCA or a main steam line break accident.

   1. Describe the testing program by which the opening characteristics of the foils, doors and dampers assumed in the analyses will be verified.

   2. In the absence of containment atmospheric sprays and fan coolers, the containment internal heat structures (heat sinks) play a vital role in removing steam from the containment atmosphere following a high energy line break within containment. The expected heat sink inventory is given in FSAR Table 6.2.1.5. Describe the pre-operational inspections which will be performed to ensure that the heat sinks given in Table 6.2.1.5 are present in the as built plant.

   3. Section 6.2.2 of the FSAR contends that long-term hydrogen mixing experiments at the Battelle Model Containment (BMC) facility show that adequate containment mixing will occur under post-LOCA conditions at EPR. At BMC flashing of superheated liquid in the containment sump was reported to be the agent for containment mixing. FSAR Section 6.2.1.1.3 describes how following a LOCA subcooled water spills out of the postulated break on to the heavy floor

and into the IRWST promoting steam condensation. The staff does not understand how the same water source can provide both heating and cooling. Describe this process in greater detail and provide justification that the processes which occurred at the test facility will occur at EPR. Provide a scaling analysis of the BMC and EPR containments to demonstrate that it is appropriate to apply BMC test results to the EPR.

d. Containment Compartments and Flow Paths (FSAR Section 6.2.1.1.2)

1. Additional Flow Paths

From examining FSAR Figures 3.8-1 through 3.8-13, the NRC staff is concerned that significant flow paths might have been omitted form Table 6.2.1-07-3. For example: The vertical grating openings from UJA rooms 15-003 to 18-003 (elevation +30.77 ft) and from 23-003 to 29-003 (elev +64.8 ft) are included in Table 6.2.1-07. There should also be openings from room 11-003 to 15-003 (elev +17 ft) and from 18-003 to 23-003 (elev +45 ft) because the steam generator rooms form a vertical stack. We believe that the flow paths described in the attached Tables 1 and 2 may exist. Provide data for elevation, opening type and area for these flow paths or provide justification that the flow paths do not exist or are insignificant. For initially closed doors, flaps and dampers provide the differential pressure required to open.

2. Room volumes:

The Reactor Building rooms of US-EPR are identified in FSAR Figures 3.8-1 through 3.8-13. Table 6.2.1-07-02 of RAI 6.2.1 lists the elevation and free volumes of these rooms. The staff could not find UJA rooms 15-026, 15-027, 18-026, 18-027, 23-026, 23-027, 29-025 and 29-026 from the Chapter 3.8 figures on the table. Does Areva believe that these rooms will not affect the results from multi-noded containment analyses of design basis accidents? If not, provide information for these rooms similar to that of Table 6.2.1-07-02 including the associated containment heat structures. Otherwise the staff will leave them out of the multi-noded containment model which we are building.

3. Opening direction of doors:

The pressure differentials required to open the doors between the UJA rooms in FSAR figures 3.8-1 through 3.8-13 are identified in Table 6.2.1-07-03 of RAI 6.2.1. Should the staff assume that the doors are able to open only to positive direction (one-way opening), or should we model the doors as opening to both directions? If the doors are capable of opening in the reverse opening direction provide the reverse opening pressures.

Table 1. Continuously open connections.

From room	To room
07017	04002
04003	07016
04004	07019
04005	07022

04006 07023
04012 07012
07012 11012
07013 11020
07017 11022
07018 07014
07020 07023
07020 07028
07021 07027
07022 07021
07023 11024
07024 07020
07024 07022
07024 07027
07026 07023
07026 11024
07028 07027
07028 07027
07028 11023
07029 07026
07029 07028
07029 11024
11002 11003
11002 15002
11003 15003
11004 11005
11004 15004
11005 15005
11006 11007
11006 15006
11007 15007
11008 11009
11008 15008
11009 15009
11010 15010
11012 15012
11013 15013
11014 11013
11014 15014
11015 11016
11015 15015
11016 15016
11019 15019
11019 15018
11021 15025
11021 11002
11021 11023
11021 07021
11022 11023
11023 07028

11024 11009
11024 11023
11031 11025
11031 11026
11032 11027
11032 11028
15001 15017
15010 18010
15011 18011
15012 18012
15013 15014
15013 18013
15014 18014
15015 15016
15015 18015
15016 18016
15018 15019
15018 18018
15019 18019
15020 15021
15023 29013
15026 18026
15027 18027
18002 18003
18002 23002
18003 23003
18004 18005
18004 23004
18005 23005
18006 23006
18007 18006
18007 23007
18008 23008
18009 18008
18009 23009
18010 23010
18011 23011
18012 23012
18013 18014
18013 23013
18014 23014
18015 18016
18015 23015
18016 23016
18018 18019
23002 23003
23004 23005
23006 23007
23009 23008
23010 29023

23011 29011
23012 29012
23013 23014
23014 29023
23015 23016
23017 11003
23018 11008
23019 29019
23042 23014
29003 29004
29003 34003
29004 29005
29004 34004
29005 34005
29006 34006
29007 29006
29007 34007
29008 29007
29008 34008
29011 34011
29012 34012
29013 40001
29016 40001
29013 29016
29014 29018
29014 34014
29015 34015
29019 34019
34003 34004
34003 23017
34004 34005
34007 34006
34008 34007
18025 18013
15014 15026
15015 15027
34020 29020
34021 29021
34018 23018

Table 2. Doors.

From room To room
07019 07018
07026 07023
07027 07022
07028 07024
11019 11018
11021 11013
11031 11014

11032 11015
15014 15026
15015 15027
15020 15013
15024 15001
15025 15013
15026 15014
15027 15015
18002 18025
18014 18026
18015 18027
18025 18013
23002 23020
23009 23031
23014 23026
23015 23027
23017 23026
23042 23014
29022 29015
34014 34018
34020 34014

34021 34015

Response to Question 06.02.01-12:

a. Steam Line Break Calculations (FSAR Section 6.2.1.1.3)

1) U.S. EPR FSAR main steam line break (MSLB) analyses of record considered initial power levels of 0%, 20%, 50%, 80%, and 100%, with the limiting case being a double-ended MSLB from 50% power. All of these analyses were repeated with additional analyses from initial power levels of 40% and 60% to demonstrate that the power level producing the most severe containment results has been identified. The results of the analyses demonstrate that there is little difference in the peak containment pressure for double-ended guillotine breaks from 50%, 60%, and 80% initial power and that the limiting peak containment pressure is 65.1 psia from a double-ended guillotine break from 60% power, as shown in Table 06.02.01-12.a.1-1. The results also indicated a slightly lower peak containment pressure than is reported in the FSAR. Since the FSAR results are more severe, no revision to the FSAR was made at this time. The FSAR will be updated in response to RAI 209, question 06.02.01-14, using a multi-noded GOTHIC model by December 18, 2009.

Table 06.02.01-12.a.1-1—Peak Containment Pressure from Double Ended Guillotine Break

Initial Power	Peak Containment Pressure (psia)
100%	63.0
80%	65.0
60%	65.1
50%	65.0
40%	62.7
20%	59.1
0%	59.9

The containment response to the MSLB was calculated using the single-node GOTHIC model. The MSLB multi-node GOTHIC model is under development, and when completed will be used to reanalyze the MSLB containment response. Use of the MSLB multi-node GOTHIC model will require an update to the U.S. EPR FSAR.

2) All break sizes from all initial power levels have been reanalyzed and extended to 30 minutes (1800 seconds), the time at which operator action is credited with isolating emergency feedwater flow. In all cases, the maximum containment pressure occurred prior to the end of the transient, with the latest peak occurring at approximately 610 seconds for the 0.5 ft² break from 20% initial power

   The containment response to the MSLB was calculated using the single-node GOTHIC model. The MSLB multi-node GOTHIC model is under development, and when completed will be used to reanalyze the MSLB containment response. The use of the MSLB multi-node GOTHIC model will require an update to the U.S. EPR FSAR.

3) The calculated containment vapor temperature for some MSLB cases exceeds the specified containment design temperature of 338ºF for a short period of time. While the analyses show the vapor space is superheated, the containment walls and structures are not. Condensation on the building surfaces is the primary heat transfer mode during this time. Therefore, the building surface temperature will be no greater than the saturation temperature at the building design pressure of 62 psig, or 309.1ºF.

   Equipment installed in containment is qualified for MSLBs in accordance with U.S. EPR FSAR, Tier 2, Chapter 3, Appendix 3D, Figure 3D-1, which envelopes the maximum expected containment MSLB temperature.

c. Containment Atmospheric Mixing and Heat Transfer Modeling (FSAR Section 6.2.1.1.3)

1) The full spectrum of loss of coolant accident (LOCA) and MSLB containment analyses will be analyzed with a multi-node GOTHIC model that employs the GOTHIC Diffusion Layer Model (DLM). The Diffusion Layer Model includes convection heat transfer and condensation models that are described in Section 9.1.6 of the GOTHIC Technical

Manual. The DLM option allows the user to specify heat sink orientation to establish the wall source terms that determine the heat transfer coefficients. The DLM option is based on well-established principles of the heat and mass transfer analogy and has been accepted by the NRC for containment integrity analysis. The heat sinks in the U.S. EPR multi-node GOTHIC containment model will include three possible orientations: vertical, horizontal facing up (e.g., floors) or horizontal facing down (e.g., ceilings).

2) A response to this question was provided in RAI-82 Response Supplement 1.

3) A complete response to this question will be provided by December 18, 2009.

Partial opening of the convection and rupture foils and the hydrogen mixing dampers will be addressed as part of the multi-node GOTHIC small break LOCA (SBLOCA) and MSLB analyses. The SBLOCA analysis will include sensitivities on the available vent area and opening properties of the foils. The operation of the hydrogen mixing dampers is governed by the instrumentation and control system and subject to the event single failure criterion. Sensitivity studies will be performed with all doors closed, all doors open, and combinations in between. Doors specific to the pressurizer compartment will be addressed as part of the response to RAI 221, Question 06.02.01-15.30.

3-1. Components of the CONVECT sub-system are undergoing a rigorous proof-of-concept and qualification testing program designed to verify their operability characteristics. The tests are designed to verify the operability of the components under the environmental conditions for which they are designed. Test criteria and conditions are established to verify their opening characteristics and their integrity under varying operating environments.

The qualification program for the convection and rupture foils uses a multifaceted approach to simulate their operating environment. Since the foils are an integral part of the two-room containment strategy and must maintain leak tightness during normal operation of the plant, environmental conditions (radiological and thermal) corresponding to a 60 year life span are simulated in radiological and thermal aging tests. In addition, the foils are seismically tested. After radiological aging and seismic testing, the sample foils are tested for leak tightness before undergoing thermal aging. Another leak tightness test is performed before submitting the samples to a load cycle test to prove resistance to small pressure fluctuations caused by normal heating, ventilation, and air conditioning (HVAC) operation. A final leak tightness test concludes the normal operating conditions testing program. The next set of tests focuses on rupturing and thermal opening of the rupture and convection foils, respectively. Several different types of tests confirm their opening under several different temperature and pressure rise scenarios.

The hydrogen mixing dampers undergo a similar qualification program. In this case the actuator and damper are exposed to environmental conditions simulating a 60 year life span. These thermal and radiation aging tests demonstrate the operability of the hydrogen mixing dampers under normal plant environmental conditions, with the performance characteristics of the dampers measured before and after aging. To simulate a seismic event and to confirm the operability of the dampers following such an event, the assembled mixing dampers are installed on a “shaker” table to reproduce the effects of an airplane impact or earthquake. Finally, the mixing dampers undergo a reliability and LOCA test. The former test verifies that the hydrogen mixing damper actuator operates reliably under long-term open-close cycles, while the latter test verifies operation under the extreme pressure and temperature conditions of a LOCA.

The design of the doors and their opening characteristics will be specified later in the design process. An appropriate qualification program will be established to verify the analyses and design assumptions.

3-2. An ITAAC has been prepared to confirm the minimum heat sink surface area value after construction. U.S. EPR FSAR, Tier 1, Section 2.1.1.1, Item 2.14 and Table 2.1.1-8, Item 2.14 will be added to require that deviations between as-built construction drawings and dimensions used in the containment analyses have been reconciled.

U.S. EPR FSAR, Tier 2, Section 6.2.1.1.3 will be revised to indicate the minimum heat sink surface area value (64,998 m^2 or 699,633 ft^2). U.S. EPR FSAR, Tier 2, Table 6.2.1-5 will be revised to indicate the cumulative available surface area (67,646 m^2 or 728,136 ft^2) and the minimum surface area (64,998 m^2 or 699,633 ft^2).

3-3. The BMC Test referenced in U.S. EPR FSAR Tier 2, Section 6.2.2 was part of the Biblis Rx series of tests. AREVA NP Technical Report ANP-10299P, Sections 6.2.2.6 and 6.2.2.7, benchmark both the single-node and multi-node GOTHIC models to this test series. At the beginning of the BMC test the liquid in the sump is subcooled. As the test proceeds, a heater in the sump is activated which increases the temperature of the sump liquid above the saturation temperature at the vapor partial pressure. Vapor then rises from the pool into the dome region where it condenses on the concrete heat sinks. The test showed that the steam production from the sump enhances the circulation in the test containment.

The U.S. EPR containment analyses show analogous behavior to the Biblis Rx tests. The IRWST is initialized at 122ºF which is below the saturation temperature at the vapor partial pressure. As such, the surface of the IRWST is capable of condensing steam at the interface between the liquid and the vapor. As the event progresses, saturated liquid spilling from the break and condensate from the heat sinks recirculate to the IRWST, which in turn increases the IRWST temperature. As the temperature of the IRWST increases the containment pressure begins to decrease. The point at which the IRWST temperature exceeds the saturation temperature at the vapor partial pressure indicates a transition from condensation to vaporization at the IRWST surface.

For comparison, the peak IRWST temperature for emergency core cooling system pump net positive suction head considerations was 230ºF at approximately 12,000 seconds. This corresponds to the saturation temperature at the vapor partial pressure of approximately 35 psia. The containment total pressure was approximately 25 psia at 12,000 seconds in this case, which would make the surface of the IRWST vaporize into the containment until the temperature matches the saturation conditions.

The liquid-to-vapor interface of the IRWST is deactivated in the U.S. EPR multi-node GOTHIC model. Figure 06.02.01-12.c.3-3-1 supports the IRWST liquid temperature calculated in the U.S. EPR FSAR, and Figure 06.02.01-12.c.3-3-2 supports the containment total pressure calculated in the U.S. EPR FSAR.

The scaling analysis that validates the phenomena important to the containment analysis will be provided in the next revision of AREVA NP Technical Report ANP-10299 which will be submitted by July 31, 2009.

Figure 06.02.01-12.c.3-3-1—Hot Leg LOCA Primary Containment Liquid Temperatures

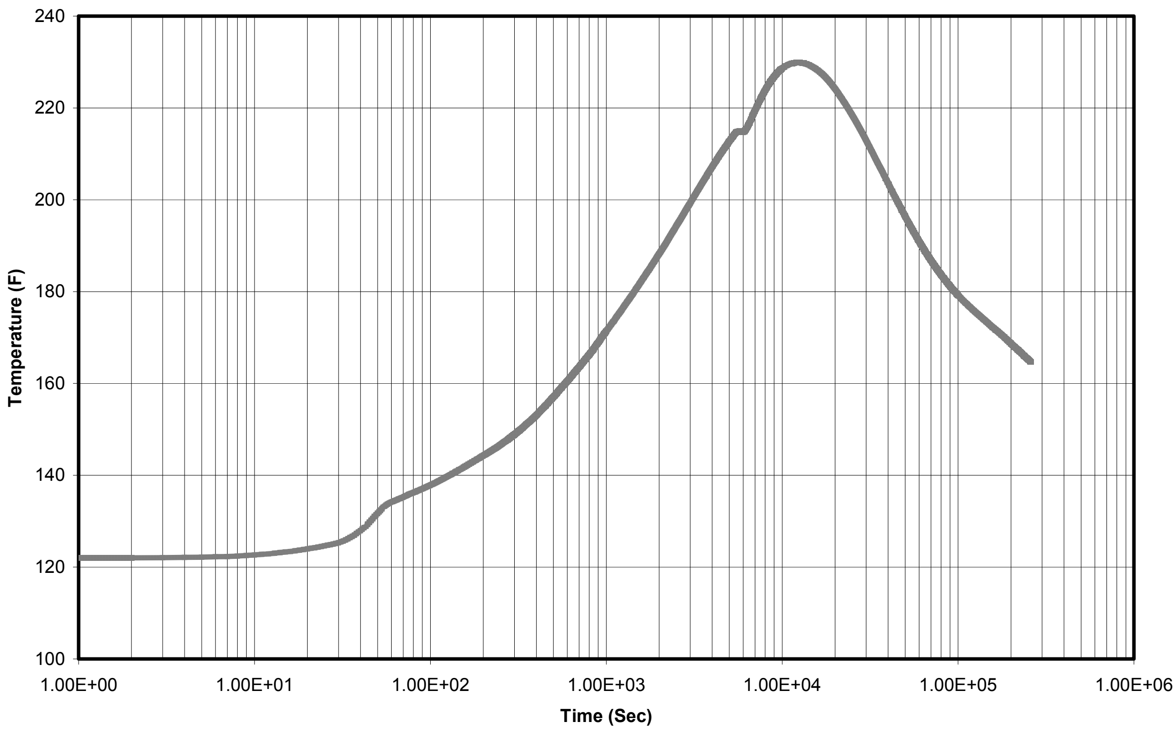

Figure 06.02.01-12.c.3-3-2— Hot Leg LOCA Primary Containment Pressure

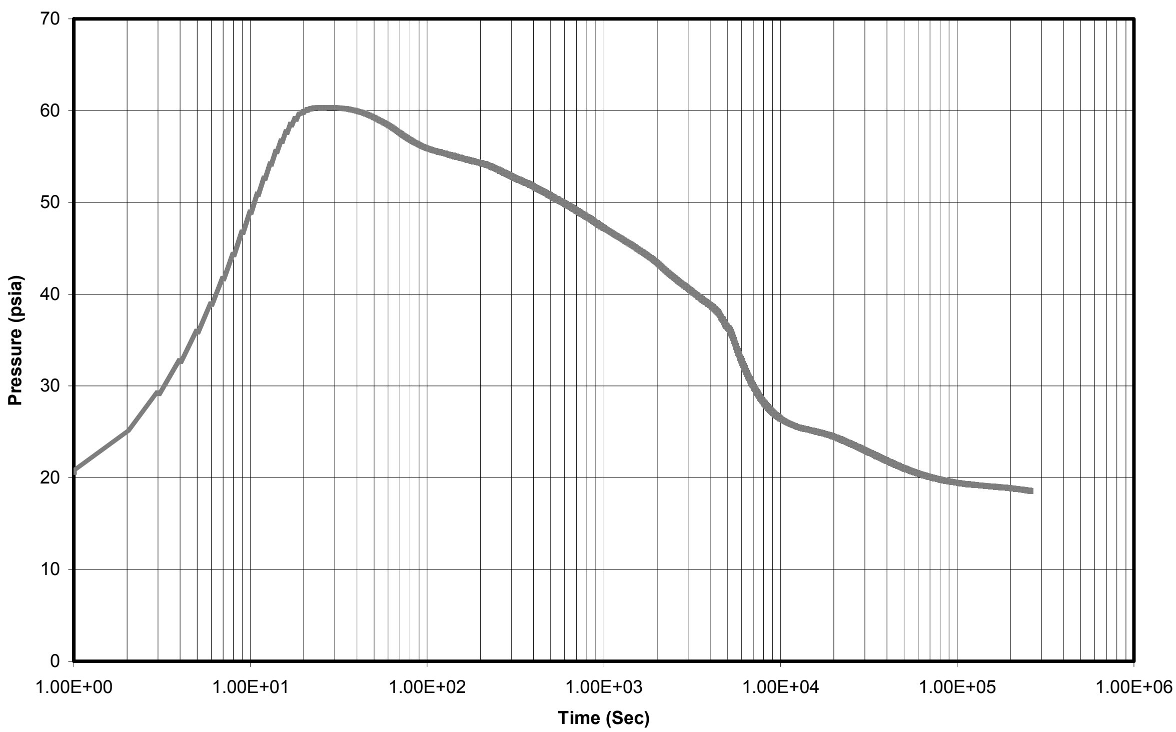

d. Containment Compartments and Flow Paths (FSAR Section 6.2.1.1.2)

1. Additional Flow Paths

The flow paths listed in Tables 1 and 2 of the question are omitted in Table 6.2.1-07-3 of AREVA NP's RAI 1 response to question 06.02.01-07c for one or more of the following reasons:

1) Flow path is internal to a control volume
2) Connecting room is not included in the containment model
3) Connecting room does not exist or is mislabeled
4) Physical connection does not exist (or is insignificant)

An item-by-item disposition of the flow paths listed in Tables 1 and 2 of the question is given below in Table 6.2.1-12.d.1. A brief discussion of each of the above reasons follows:

1) Table 6.2.1-07-3 of the response to RAI 1 question 06.02.01-07c contains only the flow paths that connect the control volumes used in the multi-node containment model. Since a control volume consists of one or more rooms, the

flow paths connecting the constituent rooms are not listed because they are internal to the control volume. For example, the flow path from room 11-003 to 15-003 is not listed because these rooms are part of the same control volume (CV3). Similarly, the flow path from room 18-003 to 23-003 is not listed because these rooms are part of the control volume CV5. Of the 172 flow paths listed in Tables 1 and 2, 146 are in this category.

2) The multi-node containment model intentionally excludes the elevator and the HVAC shafts. These rooms are small relative to the adjacent rooms and do not contain any high energy lines. Accordingly, flow paths connected to these rooms are also not listed in Table 6.2.1-07-3 of the response to RAI 1 question 06.02.01-07c. Twelve of the flow paths listed in Tables 1 and 2 are in this category.

3) Rooms 18-025, 29-020, 29-021, 34-020, and 34-021 are not in U.S. EPR FSAR, Tier 2, Figures 3.8-1 through 3.8-13. Five of the flow paths listed in Tables 1 and 2 connect to one of more of these rooms. AREVA was unable to locate the following rooms that were listed in Tables 1 and 2 of question 06.02.01-12.d.1 on U.S. EPR FSAR Figures 3.8-1 through 3.8-13: 18-025, 29-020, 29-021, 34-020 and 34-021.

4) There are twelve flow paths that are listed in Tables 1 and 2 that cannot be identified in U.S. EPR FSAR, Tier 2, FSAR Figures 3.8.-1 thru 3.8-13. These flow paths are annotated in the remarks column of Table 6.2.1-12.d.1 by, "*There is no direct connection between these rooms*." The rooms associated with these flow paths do not have any physical connection except the flow path from room 11-021 to 07-021. This is a small pipe chase with negligible flow area and it has been neglected in the containment model.

2. Room volumes:

The UJA rooms 15-026, 15-027, 18-026, 18-027, 23-026, 23-027, 29-025, and 29-026 are HVAC shafts with small volume and no high energy lines. They have not been included in the multi-node containment model because their effect on the results is insignificant.

3. Opening direction of doors:

The subcompartment analysis discussed in U.S. EPR FSAR, Tier 2, Section 6.2.1 treats all doors as uni-directional. That, is the doors are allowed to pass flow only in the positive direction. Currently, all U.S. EPR doors are under review for the direction of burst; the status of this review is as follows.

- The doors listed in Table 6.2.1-07-03 of AREVA NP's original response to RAI 1 question 6.2.1-7c that serve a radiation protection function can only open in the positive direction (one-way opening). (The positive direction is toward the "To" room in the Table.) These doors are listed separately in Table 6.2.1-12.d.3 extracted from AREVA NP's original response to RAI 40 question 06.02.01-11.5, Table 6.2.1-11-3. This is also the opening direction shown in U.S. EPR FSAR, Tier 2, Figures 3.8-1 through 3.8-13.

- For the remaining doors, the area and positive direction of the connecting vent paths for the evaluation of the short-term pressure increase and the opening of doors and blowout panels to relieve this pressure will be confirmed later in the design process in accordance with U.S. EPR FSAR Tier 1, Table 2.1.1-4 Item 3.4 for pipe break hazards (refer to AREVA NP RAI 132 Response Supplement 1, question 14.03.02-11).

Table 6.2.1-12.d.1—Flow Paths Omitted in Multi-Node Containment Model

Room		Control Volume		Remarks
From	To	From	To	
Table 1: Continuously Open Connections				
07-017	04-002	1	1	Internal flow path
04-003	07-016	2	30	There is no direct connection between these rooms.
04-004	07-019	18	18	Internal flow path
04-005	07-022	17	17	Internal flow path
04-006	07-023	17	17	Internal flow path
04-012	07-012	29	29	Internal flow path
07-012	11-012	29	29	Internal flow path
07-013	11-020	26	26	Internal flow path
07-017	11-022	1	17	There is no direct connection between these rooms.
07-018	07-014	18	19	There is no direct connection between these rooms.
07-020	07-023	17	17	Internal flow path
07-020	07-028	17	17	Internal flow path
07-021	07-027	17	17	Internal flow path
07-022	07-021	17	17	Internal flow path
07-023	11-024	17	17	Internal flow path
07-024	07-020	17	17	Internal flow path
07-024	07-022	17	17	Internal flow path
07-024	07-027	17	17	Internal flow path
07-026	07-023	17	17	Internal flow path
07-026	11-024	17	17	Internal flow path
07-028	07-027	17	17	Internal flow path
07-028	07-027	17	17	Internal flow path
07-028	11-023	17	17	Internal flow path
07-029	07-026	17	17	Internal flow path
07-029	07-028	17	17	Internal flow path
07-029	11-024	17	17	Internal flow path
11-002	11-003	3	3	Internal flow path
11-002	15-002	3	3	Internal flow path
11-003	15-003	3	3	Internal flow path
11-004	11-005	4	4	Internal flow path
11-004	15-004	4	4	Internal flow path
11-005	15-005	4	4	Internal flow path
11-006	11-007	10	10	Internal flow path
11-006	15-006	10	10	Internal flow path
11-007	15-007	10	10	Internal flow path
11-008	11-009	11	11	Internal flow path
11-008	15-008	11	11	Internal flow path
11-009	15-009	11	11	Internal flow path
11-010	15-010	27	27	Internal flow path
11-012	15-012	29	29	Internal flow path
11-013	15-013	21	21	Internal flow path
11-014	11-013	21	21	Internal flow path

Room		Control Volume		Remarks
From	To	From	To	
11-014	15-014	21	21	Internal flow path
11-015	11-016	22	22	Internal flow path
11-015	15-015	22	22	Internal flow path
11-016	15-016	22	22	Internal flow path
11-019	15-019	15	15	Internal flow path
11-019	15-018	15	15	Internal flow path
11-021	15-025	21	21	Internal flow path
11-021	11-002	21	3	There is no direct connection between these rooms.
11-021	11-023	21	17	There is no direct connection between these rooms.
11-021	07-021	21	17	Small pipe chase, neglected.
11-022	11-023	17	17	Internal flow path
11-023	07-028	17	17	Internal flow path
11-024	11-009	17	11	There is no direct connection between these rooms.
11-024	11-023	17	17	Internal flow path
11-031	11-025	21	21	Internal flow path
11-031	11-026	21	21	Internal flow path
11-032	11-027	22	22	Internal flow path
11-032	11-028	22	22	Internal flow path
15-001	15-017	9	9	Internal flow path
15-010	18-010	27	27	Internal flow path
15-011	18-011	28	28	Internal flow path
15-012	18-012	29	29	Internal flow path
15-013	15-014	21	21	Internal flow path
15-013	18-013	21	21	Internal flow path
15-014	18-014	21	21	Internal flow path
15-015	15-016	22	22	Internal flow path
15-015	18-015	22	22	Internal flow path
15-016	18-016	22	22	Internal flow path
15-018	15-019	15	15	Internal flow path
15-018	18-018	15	15	Internal flow path
15-019	18-019	15	15	Internal flow path
15-020	15-021	21	21	Internal flow path
15-023	29-013	25	25	Internal flow path
15-026	18-026			"To" room is an HVAC shaft and not modeled
15-027	18-027			"To" room is an HVAC shaft and not modeled
18-002	18-003	5	5	Internal flow path
18-002	23-002	5	5	Internal flow path
18-003	23-003	5	5	Internal flow path
18-004	18-005	6	6	Internal flow path
18-004	23-004	6	6	Internal flow path
18-005	23-005	6	6	Internal flow path
18-006	23-006	12	12	Internal flow path
18-007	18-006	12	12	Internal flow path
18-007	23-007	12	12	Internal flow path
18-008	23-008	13	13	Internal flow path

Room		Control Volume		Remarks
From	To	From	To	
18-009	18-008	13	13	Internal flow path
18-009	23-009	13	13	Internal flow path
18-010	23-010	27	27	Internal flow path
18-011	23-011	28	28	Internal flow path
18-012	23-012	29	29	Internal flow path
18-013	18-014	21	21	Internal flow path
18-013	23-013	21	21	Internal flow path
18-014	23-014	21	21	Internal flow path
18-015	18-016	22	22	Internal flow path
18-015	23-015	22	22	Internal flow path
18-016	23-016	22	22	Internal flow path
18-018	18-019	15	15	Internal flow path
23-002	23-003	5	5	Internal flow path
23-004	23-005	6	6	Internal flow path
23-006	23-007	12	12	Internal flow path
23-009	23-008	13	13	Internal flow path
23-010	29-023	27	27	Internal flow path
23-011	29-011	28	28	Internal flow path
23-012	29-012	29	29	Internal flow path
23-013	23-014	21	21	Internal flow path
23-014	29-023	21	27	There is no direct connection between these rooms
23-015	23-016	22	22	Internal flow path
23-017	11-003	5	3	There is no direct connection between these rooms
23-018	11-008	13	11	There is no direct connection between these rooms
23-019	29-019	16	16	Internal flow path
23-042	23-014	21	21	Internal flow path
29-003	29-004	7	7	Internal flow path
29-003	34-003	7	7	Internal flow path
29-004	29-005	7	7	Internal flow path
29-004	34-004	7	7	Internal flow path
29-005	34-005	7	7	Internal flow path
29-006	34-006	14	14	Internal flow path
29-007	29-006	14	14	Internal flow path
29-007	34-007	14	14	Internal flow path
29-008	29-007	14	14	Internal flow path
29-008	34-008	14	14	Internal flow path
29-011	34-011	28	28	Internal flow path
29-012	34-012	29	29	Internal flow path
29-013	40-001	25		Internal flow path
29-016	40-001	25		Internal flow path
29-013	29-016	25	25	Internal flow path
29-014	29-018	23	23	Internal flow path
29-014	34-014	23	23	Internal flow path
29-015	34-015	24	24	Internal flow path
29-019	34-019	16	16	Internal flow path

Room		Control Volume		Remarks
From	To	From	To	
34-003	34-004	7	7	Internal flow path
34-003	23-017	7	5	There is no direct connection between these rooms
34-004	34-005	7	7	Internal flow path
34-007	34-006	14	14	Internal flow path
34-008	34-007	14	14	Internal flow path
18-025	18-013		21	Room 18-025 not in FSAR Figures 3.8-1 through 3.8-13
15-014	15-026	21		"To" room is an HVAC shaft and not modeled
15-015	15-027	22		"To" room is an HVAC shaft and not modeled
34-020	29-020			Rooms 34-020 and 29-020 not in FSAR Figures 3.8-1 through 3.8-13
34-021	29-021			Rooms 34-021 and 29-021 not in FSAR Figures 3.8-1 through 3.8-13
34-018	23-018	23	13	There is no direct connection between these rooms
Table 2: Doors				
07-019	07-018	18	18	Internal flow path
07-026	07-023	17	17	Internal flow path
07-027	07-022	17	17	Internal flow path
07-028	07-024	17	17	Internal flow path
11-019	11-018	15	15	Internal flow path
11-021	11-013	21	21	Internal flow path
11-031	11-014	21	21	Internal flow path
11-032	11-015	22	22	Internal flow path
15-014	15-026	21		"To" room is an HVAC shaft and not modeled
15-015	15-027	22		"To" room is an HVAC shaft and not modeled
15-020	15-013	21	21	Internal flow path
15-024	15-001	9	9	Internal flow path
15-025	15-013	21	21	Internal flow path
15-026	15-014		21	"From" room is an HVAC shaft and not modeled
15-027	15-015		22	"From" room is an HVAC shaft and not modeled
18-002	18-025	5		Room 18-025 does not exist
18-014	18-026	21		"To" room is an HVAC shaft and not modeled
18-015	18-027	22		"To" room is an HVAC shaft and not modeled
18-025	18-013		21	Room 18-025 does not exist
23-002	23-020	5	5	Internal flow path
23-009	23-031	13	13	Internal flow path
23-014	23-026	21		"To" room is an HVAC shaft and not modeled
23-015	23-027	22		"To" room is an HVAC shaft and not modeled
23-017	23-026	5		There is no direct connection between these rooms
23-042	23-014	21	21	Internal flow path
29-022	29-015	24	24	Internal flow path
34-014	34-018	23	23	Internal flow path
34-020	34-014		23	Rooms 34-020 not in FSAR Figures 3.8-1 through 3.8-13
34-021	34-015		24	Rooms 34-021 not in FSAR Figures 3.8-1 through 3.8-13

Table 6.2.1-12.d.3—Radiation Protection Doors – Uni-Directional

Junction Number	From Connection		To Connection	
	Control Volume	Room (30UJA)	Control Volume	Room (30UJA)
18	3	15-002	21	15-025
18	3	15-003	21	15-013
22	4	11-004	21	11-031
23	4	15-004	21	15-014
23	4	15-005	21	15-014
26	5	23-020	21	23-013
30	6	18-004	21	18-014
30	6	18-005	21	18-014
30	6	23-005	21	23-014
33	7	29-005	23	29-018
33	7	34-005	23	34-018
38	9	15-024	15	15-018
42	10	11-007	22	11-032
43	10	15-006	22	15-015
43	10	15-007	22	15-015
45	11	15-008	22	15-016
45	11	15-009	22	15-016
48	12	18-006	22	18-015
48	12	18-007	22	18-015
48	12	23-006	22	23-015
50	13	23-031	22	23-016
51	13	18-009	22	18-016
54	14	29-006	24	29-015
54	14	34-006	24	34-015
58	15	11-018	21	11-014
60	15	18-018	21	18-014
59	15	11-018	22	11-015
61	16	23-019	21	23-042
61	16	23-041	21	23-042
63	16	29-019	24	29-015
65	17	11-023	22	11-016
64	17	07-021	30	07-016
69	19	07-014	26	07-013
72	20	07-015	26	07-013

FSAR Impact:

The U.S. EPR FSAR, Tier 1, Section 2.1.1.1 and Table 2.1.1-8 will be revised as described in the response and indicated on the enclosed markup.

The U.S. EPR FSAR, Tier 2, Section 6.2.1.1.3 and Table 6.2.1-5 will be revised as described in the response and indicated on the enclosed markup.

Question 06.02.01.02-1:

a. Conservativeness of Differential Pressure Calculations (Relates to SRP Section 6.2.1.2)

Provide the following information concerning the subcompartment differential pressure calculations:

1. Provide additional justification that the use of the homogeneous equilibrium model (HEM) is conservative for the prediction of break flow for subcompartment analysis. The response to RAI 6.2.1-08 states that the results of an EPRI study concludes that for L/D>1.5, HEM shows good agreement with test data. Provide a comparison of the L/D for the assumed breaks in the EPR subcompartment analyses with those of the test series to show that the postulated break locations for EPR fall with the range of data from which the EPRI observations were made and show that use of HEM is conservative.

2. The operating temperature used for the SIS/RHR line is 77°F, a rather low value. See FSAR tables 6.2.1.10 and 6.2.1.15. Provide justification that this low assumed operating temperature is conservative for the calculation of break mass and energy to be used in the pressurization analyses of the associated subcompartments.

3. Not all subcompartments with high energy lines were considered in the for pressure evaluation. Only those that were calculated to undergo the highest concentrated loading conditions in FSAR Chapter 3 were evaluated. Justify the omission of other subcompartments with high energy lines. What would be the consequences if the design pressure were exceeded in these subcompartments?

4. The initial conditions (e.g. containment pressure, temperature, relative humidity) at the receiving node and surrounding nodes were said to be imposed to maximize the resultant differential pressure across the affected node. All initial conditions for each subcompartment were not presented. Table 6.2.1-4 in FSAR Tier 2 lists the overall containment initial conditions. Section 6.2.1.1 (page 6.2-3), states that the initial pressure for subcompartment transient differential pressure analysis is 14.7 psia which is consistent with the pressure at time zero in Figures 6.2.1-5 through 6.2.1-9. The selection of initial conditions should maximize the calculated differential pressure. Justify that this was done and provide the initial conditions for all subcompartments analyzed.

5. The evaluation of subcompartment pressure is dependant on the input coefficients of inertia and the flow loss coefficient. Provide and justify the method by which the flow and inertia coefficients were chosen. Values of 1.5 were used for the flow loss coefficients. Page 225 of the 1994 Handbook of Hydraulic Resistance by Idelchik indicates that the coefficient varies with the length to diameter ratio of the hole and is between 2.85 and 1.55. Provide sensitivity studies showing the effect on subcompartment pressure to uncertainty in flow loss coefficients and provide justification that the approach taken is conservative.

6. A Nodalization sensitivity study was performed by dividing each critical room circumferentially in four nodes. According to the sensitivity analysis, the circumferential

nodalization affects the local peak pressure by several psi. NUREG-0609 Chapter 3.2.2 recommends that the subcompartments be analyzed by subdividing them into a number of control volumes or nodes. Provide additional noding sensitivity studies including the effects of axial and radial noding. Discuss how the compartment pressure variations within will be included in the Chapter 3 loading evaluations and justify that this representation is conservative. Provide the sub-node volumes and flow path inputs used in the noding sensitivity studies.

7. Provide and justify to be conservative the heat transfer assumptions that are used in the GOTHIC models for subcompartment analysis.

8. The last paragraph of FSAR (Rev. 0) Section 6.2.1.2.2 (page 6.2-10), describes that the vent paths considered in the subcompartment analysis include open doors as well as grates and through wall openings. It is also stated that the effects of vent areas that become available after the occurrence of a pipe break are specifically noted and conservatively treated. Provide more details about how this is done. Tables 6.2.1-11 through 6.2.1-14 show all doors to remain closed in the analyses of critical subcompartments. Are any foils or dampers considered in the subcompartment analyses? If so their theatment should be described. Descibe the treatment of initially closed vent paths for the remander of the subcompartments that were analyzed as shown in Table 6.2.1-10.

9. FSAR Tables 6.2.1-11 through 6.2.1-14 indicate that the large lumped volumes are connected by doors to the break volume and that these doors remain closed. With only the smaller volumes considered in the analysis, one would expect pressures in the remaining volumes to trend upward as the blowdown continues. Figures 6.2.1-5 through 6.2.1-9 indicate that once the initial inertial spike is passed that the pressure in the break volume approaches an constant value. Describe the processes within the GOTHIC code which mitigate the pressure increase and justify that the analysis is conservative for determining subcompartment differential pressures.

10. Maximum calculated accident pressures are strongly affected by the area of the connecting vent paths. Describe the preoptional measures, inspections, ITAAC etc., that will be taken to ensure that the as-built subcompartments are consistent with the assumptions made in FSAR Section 6.2.1.2.

b. Subcompartment Pressure Loads (Relates to SRP Section 6.2.1.2)

1. FSAR Tier 2, Table 6.2.1-10 shows “accident pressures” for critical subcompartments but not for all listed rooms. The values shown differ from calculated pressures in FSAR Tier 2, Figures 6.2.1-5 through 6.2.1-9. What is the relation between “accident pressure” and calculated pressure? Provide the pressures calculated for all subcompartments and the pressures that are utilized in the compartment loading analyses of Chapter 3.

2. For each subcompartment for which the pressure response to a high energy pipe break was calculated, provide a comparison of the calculated subcompartment pressure with the maximum pressure allowed by the subcompartment design and justify that sufficient margin is available.

3. The subcompartment pressure analyses shown in FSAR Figures 6.2.1.5 through 6.2.1.7 show considerable variation in the peak pressure around the compartment

circumference. Discuss how the pressure variations in both time and location are considered in the Chapter 3 loading evaluations and justify that this treatment is conservative.

4. FSAR Page 3E-11, states that "the upper portion of the of the SG/RCP wing wall and SG separation wall are subject to a sub-compartment pressurization load of 20 psi." However, the calculated accident pressures in FSAR Tier 2, Table 6.2.1-10 in room UJA29-004 is 31.07 psia, which results in 16.4 psi pressure load assuming atmospheric pressure on the other side of the wall. Page 6.2-12 (FSAR Tier 2), states that a factor of 1.4 is used in peak pressure predictions which results in 23 psi pressure load in this particular subcompartment. The calculated pressure is somewhat higher than that used in the design of the structures. The design pressures of the subcompartment and how they are applied to the compartment load analyses should be clarified.

Response to Question 06.02.01.02-1:

a.1 A response to this question was provided in AREVA NP's original response to RAI 82.

a.2 Operating Temperature Used for the SIS/RHR Line (77°F)

The safety injection system / residual heat removal (SIS/RHR) line was selected as the bounding high energy line in rooms UJA11-004 and UJA11-027, based on the criterion of maximum energy discharge rate. In response to this question, the rooms listed in U.S. EPR FSAR, Tier 2, Table 6.2.1.10 were re-evaluated for bounding high-energy lines. As a result of this reevaluation, the high-energy lines for rooms 11-004 and 11-027 have changed as described below.

The bounding high-energy line for Room 11-004 is SIS/RHR line JNA20 BR001. This is an RHR suction line from the reactor coolant system (RCS) hot leg (2250 psia and 626ºF). The line contains two safety-grade isolation valves which are closed during power operation. Accordingly, only the upstream (RCS) end of a postulated break on this line is capable of discharging high-energy fluid.

The bounding high-energy line for Room 11-027 is SIS/RHR line JNG33BR001. This is a safety injection line from the accumulator. The line is at ambient temperature during power operation, but, for conservatism it has been assigned the accumulator design conditions of 815 psia and 140ºF.

Rooms 11-004 and 11-027 have been re-analyzed for sub-compartment pressurization using the approach described in U.S. EPR FSAR, Tier 2, Section 6.2.1. The resulting accident pressures and the data used in the analysis will be revised in the U.S. EPR FSAR Tier 2 Tables 6.2.1-10 and 6.2.1-15, respectively. The accident pressure for Room 11-004 is 20.8 psia, and for Room 11-027 it is 16.9 psia. The corresponding pressure differentials are well below the design pressure of these rooms.

a.3 A response to this question was provided in AREVA NP's original response to RAI 82.

a.4 A response to this question was provided in AREVA NP's original response to RAI 82.

a.5 A response to this question was provided in AREVA NP's original response to RAI 82.

a.6 A response to this question was provided in AREVA NP's original response to RAI 82.

a.7 A response to this question was provided in AREVA NP's original response to RAI 82.

a.8 A response to this question was provided in AREVA NP's original response to RAI 82.

a.9 A response to this question was provided in AREVA NP's original response to RAI 82.

a.10 As-Built Sub-compartment Preoperational Inspections

The area of the connecting vent paths will be confirmed to be consistent with the sub-compartment analyses performed later in the design process in accordance with U.S. EPR FSAR Tier 1 Table 2.1.1-4 Item 3.4 for pipe break hazards (refer to AREVA NP RAI 132 Response Supplement 1, question 14.03.02-11).

FSAR Impact:

U.S. EPR FSAR, Tier 2, Table 6.2.1-10 and Table 6.2.1-15 will be revised as described in the response and indicated on the enclosed markup.

Question 06.02.01.03-1:

RAI - 6.2.1.3-1 (Relates to FSAR Section 6.2.1.3, Mass and Energy Release Analyses for Postulated LOCAs)

a. The initial reactor power level for the LOCA mass and energy release calculations is 4612 MWt, which is the rated thermal power level plus a calorimetric uncertainty. The uncertainty is given in FSAR Tier 2, Section 6.2.1.1.3 as 0.5 percent. Describe how the 0.5 percent calorimetric uncertainty was established and justify that it is conservative for containment analysis. What uncertainties were considered in the uncertainty analysis? What values were used for the uncertainties? How were the uncertainties combined? Describe the interface requirements (COL Information Item) which will be transmitted to COL applicants to ensure that the assumed power uncertainty is maintained for the as-built plant.

b. Describe how reactor shutdown was calculated in the RELAP5 code. Was control rod entry assumed? If so provide or reference the evaluation that the control rods would insert against the forces generated by a large break LOCA. Was a stuck control rod assembly assumed in the calculations? What was the worth of the assembly?

c. Provide an evaluation of the effect of chugging in the reactor core on the mass and energy release rate. Provide the change in the steam release rate to the containment in case of a DEG hot leg break and a DEG pump suction break if chugging is eliminated from the calculations (core flow is assumed to be smooth).

d. Page vii of BAW -10252 states that the models and methods described therein follow the guidance of NUREG-0800 (SRP Section 6) where appropriate. Provide a comparison of the assumptions used in the LOCA mass and energy release calculations with the acceptance criteria listed in SRP Section 6.2.1.3. If the acceptance criteria were not followed include a description of assumptions used to replace the SRP criteria and provide justification that they are conservative for containment analysis.

e. Table 6.2.1-1 provides a summary of the assumptions for the various loss of coolantaccidents evaluated for the containment. Table 6.2.1-20 identifies the mass and energy results from a cold leg pump discharge break as long-term Case B. The staff could not find long-term Case B on table 6.2.1-1. Provide the assumptions used in this analysis.

f. Table 6.2.1-23 gives the end of core reflood as 3957 seconds for a double ended hot leg break and 4000 seconds for double ended breaks in a cold leg pump suction or discharge. These reflood times are longer than the staff is familiar with for operating plants. Generally short reflood times are conservative for containment analysis since energy is transferred to the containment at a faster rate. Provide the criteria that are used to determine the end of reflood for the US-EPR. Discuss the relationship of the reflood calculation to core quench as discussed in SRP 6.2.1.3 and justify that the results are conservative.

g. For the limiting hot and cold leg breaks provide the temperature history of the reactor system and secondary system components to indicate that the sensible heat from the reactor system and steam generators is being accounted for and is conservatively removed by the calculation. Provide initial values, those at the end of blowdown, those at the end of reflood, those at the time of peak pressure, those at the time of the switch between the RELAP5 and GOTHIC analysis and those at the end of 24 hours. Provide the assumptions made for heat transfer between the primary medal surfaces and the fluid within the reactor system that are used in the RELAP5 analysis. The staff requests similar heat transfer information for the GOTHIC reactor system model under item "m" of this RAI.

h. Section 6.2.1.3.3.2-d of the FSAR for Midland indicates that complete steam condensation as a result of the mixing of steam and water flowing together in a pipe should not be assumed below a threshold velocity as determined by test data. Describe and justify the threshold velocity model that is used in the RELAP5 and GOTHIC mass and energy models to determine steam and water mixing within the reactor system of US-EPR following a LOCA.

i. The EPR is equipped with 4 trains of safety injection. These are cross-connected so that trains 1 and 2 interconnect and trains 3 and 4 interconnect. If the break is in the loop fed by train 1, train 2 undergoes a single failure and train 3 is out for maintenance trains 1 and 4 would be available to deliver ECCS water to the core. The water injected into loop one might be lost from the break but by the cross-connects all loops would be fed. If the failure were in train 4, train 3 was out for maintence and train 2 were operable then only loops 1 and 2 would be fed with ECCS. For double ended breaks of the hot leg and at the reactor coolant pump suction and discharge evaluate various single failure possibilities for the safety injection trains to identify the worst case.

j. One factor which might affect the steam release from the reactor system is the filling of low points in the cold leg piping at the pump suction (loop seals) in the intact cold legs following a large cold leg break. With the intact loop cold legs plugged with water all steam from the core might exit from the break without mixing and being condensed with the ECCS water. The loop seals might be filled during the course of the accident by back flow of ECCS water at the pump discharge or by entrainment of liquid from the core through the steam generators. Provide an evaluation of the potential for and the effect of loop seal filling on the steam release to the containment following a postulated break at the reactor system pump suction.

k. Provide the noding diagrams for the RELAP5 simulation of the reactor system used to predict mass and energy release from large hot and cold leg breaks. Justify the noding selected is adequate.

l. At a time between 5000 seconds and 11000 seconds depending on the break location the mass and energy release calculation is switched from RELAP5 to a one node GOTHIC model. Describe the switching criteria used to determine the time of solution transfer between the RELAP5 and GOTHIC models. Describe the precautions taken to ensure that energy is conserved between the two models at the time of the switch.

m. Provide a complete description of the GOTHIC models used to predict the long term mass and energy releases for a large hot leg, cold leg pump discharge and cold leg pump suction models. Describe the location of reactor system heat structures for each break location as to whether they are wetted or not. Justify the heat transfer options used with the wetted and unwetted structures. Describe and justify the reactor core two-phase level swell model that is used.

n. For all break locations the steam flow from the break is eventually predicted to reach or approach zero in the GOTHIC simulation. The staff does not understand how the steam release could ever be zero for a break at the reactor coolant pump suction. Provide justification that the GOTHIC model is accurately evaluating the steam and water flow and condensation phenomena within the reactor system.

o. As cooler water is injected into the cold legs during the long term post reflood phase, the flow of vapor from the break may reverse so that the containment atmosphere is drawn into the reactor system. Consider the case of a double ended pump suction break. Demonstrate that reverse flow at the reactor vessel side of the break will not cause non-condensables to be drawn in from the containment so that the steam condensation effectiveness at the SIS injection locations is reduced. Under these conditions a greater than expected fraction of steam might flow directly to the containment through the steam generator side of the break than predicted if the effect of non-condensables were not modeled.

p. Provide justification for decreasing the core decay heat multiplier from 1.2 to 1.1 in the mass and energy release calculations for the long term post reflood phase.

Response to Question 06.02.01.03-1:

a. A response to this question was provided in AREVA NP's RAI 82 Response Supplement 1.

b. A response to this question was provided in AREVA NP's RAI 82 Response Supplement 1.

c. Chugging in the reactor core was observed during the reflood period for the loss of coolant accident (LOCA) events and is attributed to core flow oscillations occurring in that period. The oscillations may affect the mass and energy release, which in turn affects the containment pressure response following postulated LOCA events.

   Chugging was reported in the original U.S. EPR FSAR submittal for the hot leg and cold leg pump suction and discharge breaks. Subsequent to the FSAR analyses, AREVA NP modified the methodology for U.S. EPR containment response following LOCA events, and AREVA provided a description in Technical Report ANP-10299P, Revision 0, "Applicability of AREVA NP Containment Response Evaluation Methodology to the U.S. EPR for Large Break LOCA Analysis." AREVA NP provided a sample problem for the cold leg pump suction (CLPS) break. This response is based on the results of the CLPS sample problem presented in ANP-10299P, Revision 0.

   The observed oscillations consist of three phenomena in the analysis: cold-leg accumulator driven, downcomer liquid level (manometer), and loop oscillations. Cold-leg accumulator driven oscillations are considered important only during refill (i.e., accumulator injection). The oscillations appearing during early and late in reflood are attributed to interfacial interactions (i.e., drag and condensation).

   There are two principal fluid conditions that dominate core heat transfer during this period: reflooding rate and liquid sub-cooling. Initially, the flooding rate is high because of accumulator injection into the reactor vessel. Once the accumulator inventory is exhausted, the safety injection system—medium head safety injection (MHSI) and low head safety injection (LHSI) —provides the principle source of core coolant.

Following blowdown and refill, water enters the bottom region of the core and boils when it comes in contact with the hot fuel rods. A fraction of the liquid in the core is entrained and carried out of the reactor vessel with the steam.

The RELAP5/MOD2-B&W computer code used for this analysis has been benchmarked against data from the FLECHT-SEASET, UPTF, CCTF, and SCTF test programs. These tests bound the range of pressures, power densities, and mass fluxes typical for the large break LOCA (LBLOCA) reflood phase. The figures-of-merit for assessing liquid entrainment are core region void fractions, core temperatures, and carry-out rate fractions. RELAP5/MOD2-B&W benchmark analyses to these test programs show good agreement with the data for quench front propagation and carryout rate fraction.

Simultaneous gravity-driven reflooding of the core and the interaction of cold emergency core cooling (ECC) water with steam in the cold legs and downcomer causes both manometric and condensation-driven oscillations in flow rate and pressure. High reflood rates during accumulator discharge drive water rapidly toward the hot fuel surface, producing steam. As the steam expands, the water is pushed away from the fuel surface. The gravity head of the water in the downcomer pushes back on the steam, returning coolant to the core where it condenses steam. These manometric oscillations slowly dampen as the quench front progresses upward through the core. The interfacial drag models in RELAP5/MOD2-B&W improve the fluid distribution prediction and reduce the potential for numerically-induced oscillations in the core region.

Flooding Rate and Carry-out Rate Fractions for U.S. EPR:

The analysis presented in the U.S. EPR FSAR has the accumulators modeled to inject 140ºF water [ ] to conservatively shorten the duration of the refill phase. This causes steam condensation in the lower plenum at the same time the rapid boiling of liquid to steam in the core produces rapid core oscillations from 20 to 60 seconds. As the accumulators empty, the emergency core cooling system (ECCS) injection water continues the oscillation process but at a slower rate from 60 to 100 seconds. After 120 seconds, the core is quenched and the core flow oscillations subside. The flooding rate for the U.S. EPR for this period was 2.5 – 3 inch/s. Figure 06.02.01.03-1-1 shows the core inlet flow during the first 200 seconds for the analyses presented in the U.S. EPR FSAR and in AREVA Technical Report ANP-10299P.

The analysis presented in ANP-10299P modeled the accumulators so that [ ] (at 140ºF) and [ ]. This approach reduced the potential for condensation in the lower plenum and, thereby, lessened flow oscillations at the core inlet.

The rate of steam release into the containment has a primary effect on the containment pressure response. Figure 06.02.01.03-1-2 compares the rate of steam flow release into the containment for the U.S. EPR FSAR and ANP-10299P analyses.

Figure 06.02.01.03-1-3 shows the quench front position from the CLPS case presented in ANP-10299P; it indicates the core quenched in 120 seconds. After quench, the steam produced in the core region and the containment response are not sensitive to core flow oscillations.

Another important parameter is the core carry-out rate fraction (CRF). This is defined as the ratio of the total integrated mass flow rate at the bundle exit to the total integrated mass flow rate at the core inlet. RELAP5/MOD2-B&W has been benchmarked to the FLECHT-SEASET program tests discussed in Appendix G of AREVA NP Topical Report BAW-10166PA, Revision 5, “BEACH - Best-Estimate Analysis Core Heat Transfer - A Computer Program for Reflood Heat Transfer during LOCA.” These benchmarks highlight the performance of RELAP5/MOD2-B&W for predicting the carry-out rate fraction.

Figure 06.02.01.03-1-4 shows that the CRF for the U.S. EPR compares well with the FLECHT test data at similar flooding rates. After core quench, the CRF for U.S. EPR is slightly higher that the test data. This is conservative because it increases the energy removal rate from the core and steam generators. The peak containment pressure occurs during the post-reflood phase, about 90 minutes into the transient, just before initiation of hot leg injection. Because the observed flow oscillations occur only in the first few minutes of the transient, they do not have a significant impact on the overall containment response.

Figure 06.02.01.03-1-1: Inlet Core Flow

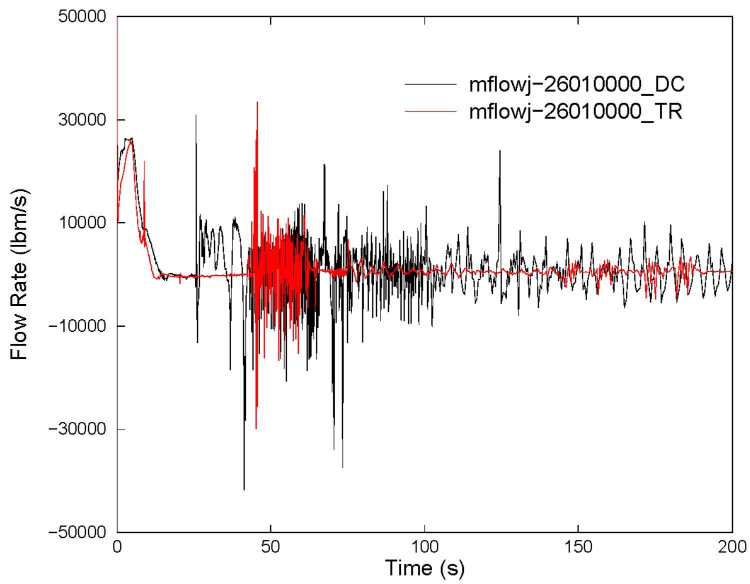

Figure 06.02.01.03-1-2: Steam Flow Release into the Containment

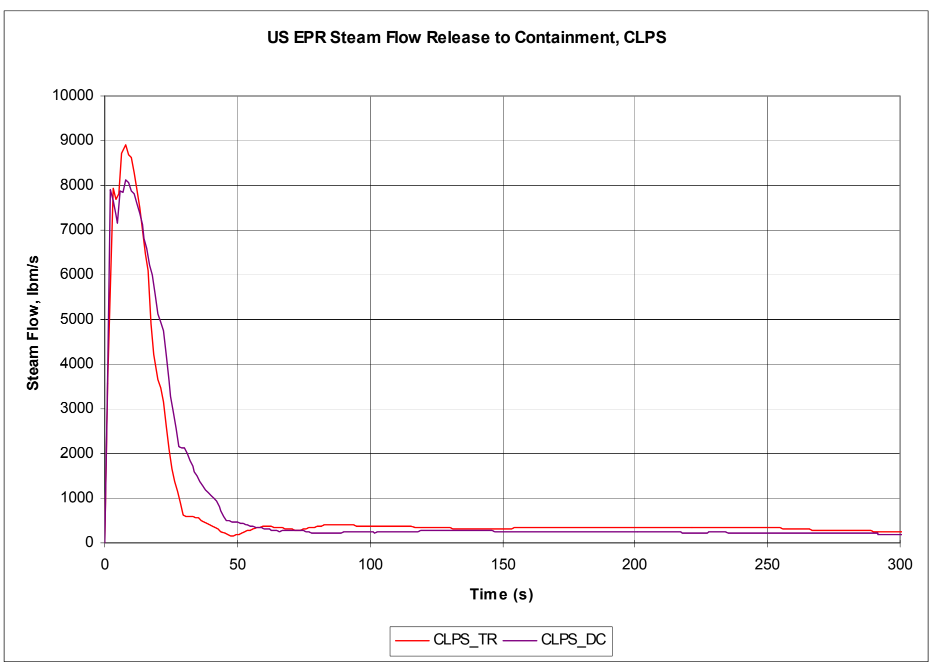

Figure 06.02.01.03-1-3: Quench Front Position

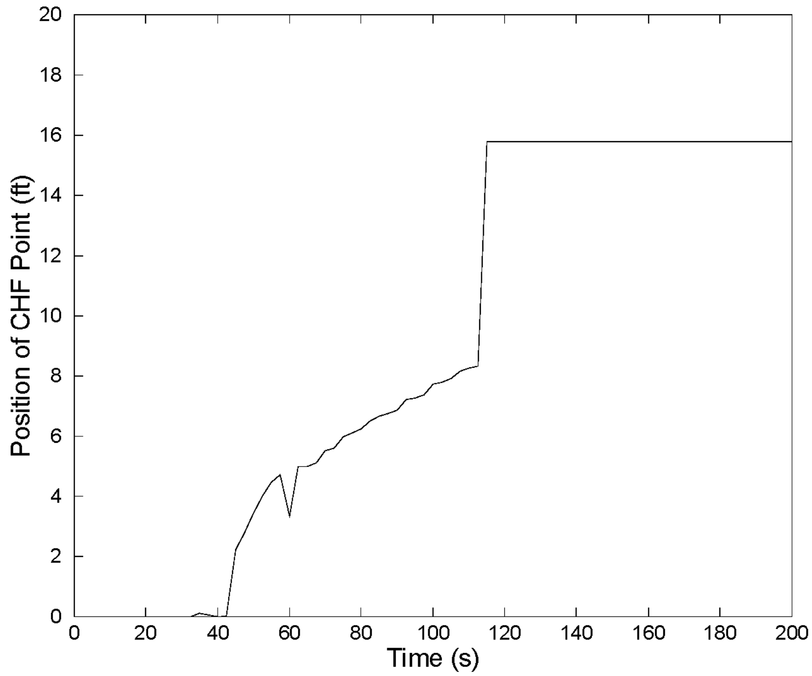

Figure 06.02.01.03-1-4: FLECHT Carryout Rate Fraction

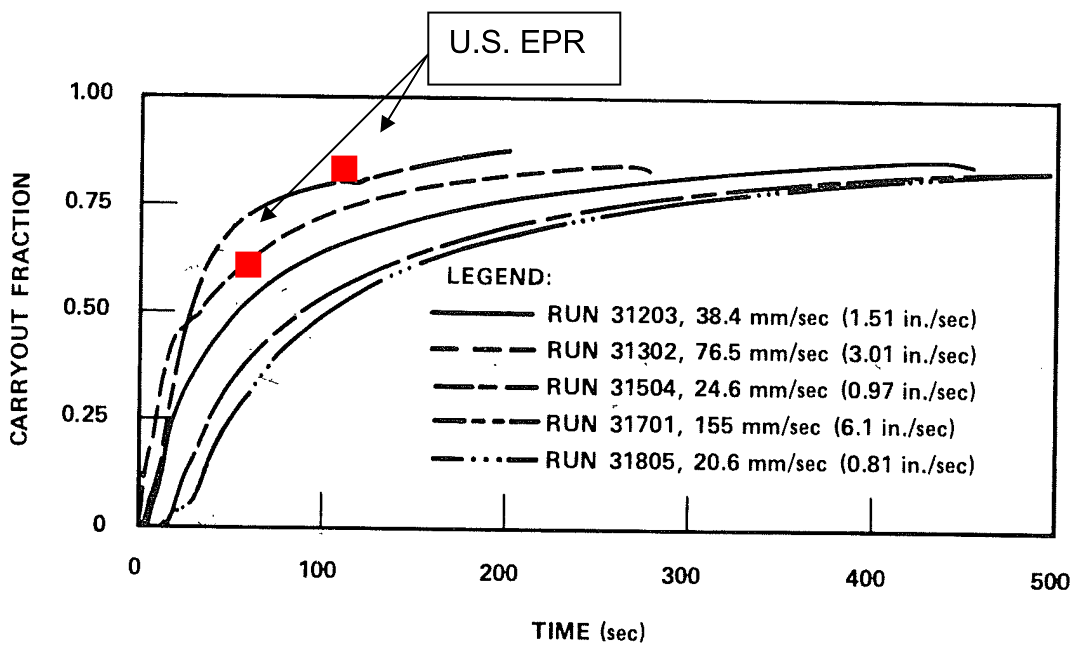

d. A response to this question was provided in AREVA NP Technical Report ANP-10299P.

e. A response to this question was provided in AREVA NP's RAI 82 Response Supplement 1.

f. A response to this question was provided in AREVA NP Technical Report ANP-10299P.

g. The hot leg and cold leg breaks that produced the limiting containment responses are described in U.S. EPR FSAR, Tier 2, Section 6.2.1. The containment response for these limiting LOCAs is evaluated from time zero until 24 hours after the postulated accident.

The short-term mass and energy (M&E) releases from these postulated LOCAs are calculated using the RELAP5/MOD2 B&W code. The long term M&E releases and the resulting containment response are calculated using the GOTHIC computer code. The short term M&E releases are used as boundary conditions to the containment response calculated with the GOTHIC code.

The temperature history information from the above analyses are reported at zero seconds, end-of-blowdown, end-of-reflood, time of peak pressure, time of switch from the RELAP5 to the GOTHIC calculations (referred to as transition time), and at the end of 24 hours into the transient.

End-of-reflood time occurs when fuel rod quench is achieved throughout the core. In addition to the end-of-reflood time, the core collapsed level is tracked until the collapsed liquid level is stable. This occurs well into the post-reflood phase. A containment energy balance is performed at this time to comply with the requirement of Table 6-15 of RG 1.206.

The AREVA NP GOTHIC methodology removes the sensible heat from the RCS metal and steam generators (SG) well before 24 hours after the LOCA. The RELAP5/MOD2 B&W computer code calculates the sensible heat dissipation mechanistically from time zero until the RELAP5-to-GOTHIC transition time. After the transition to GOTHIC, the remaining sensible heat is dissipated until the temperature of the structures reaches 120ºF. Therefore, in the AREVA NP GOTHIC methodology, the temperature history of the RCS/SG structures is known a priori at 24 hours, namely,

Structure	Structure Temperature at t = 24 hours
RCS Metal	120ºF
BLSG	120ºF
ILSG	120ºF

The sequence of events during the RELAP5 phase of the calculation is as follows:

HL LOCA Containment Response FSAR Case

Time (sec)	Event
0.0	Break opens
23.92	End-of-blowdown

26	Time of peak pressure
28	End of reflood
4000	Post-reflood time, previously selected for containment energy balance determination
5470	RELAP5 to GOTHIC transition time

The RELAP5 major edits that are available in the computer run output for this case, at or close to the above times, are as follows:

1) 0 seconds
2) 20 seconds
3) 30 seconds
4) 3957 seconds
5) 5470 seconds

As shown above, there is an exact match between sequence-of-events times and major edits only at time zero and the transition time from RELAP5 to GOTHIC. The major edit at 20 seconds is close to the end-of-blowdown time. The major edit at 30 seconds is close to the time of peak pressure and end of reflood. The major edit at 3957 seconds is close to the indicated post-reflood time.

CLPS LOCA Containment Response FSAR Case

Time (sec)	Event
0.0	Break opens
40	Time of peak pressure
50.3	End-of-blowdown
120	End of reflood
4000	Post-reflood time, previously selected for containment energy balance determination
10000	RELAP5 to GOTHIC transition time

The RELAP5 major edits that are available in the computer run output for this case, at or close to the above times, are as follows:

1) 0 seconds
2) 40.5 seconds
3) 50.5 seconds
4) 125 seconds
5) 4000 seconds
6) 10000 seconds

As shown above, there is an exact match between sequence of events times and major edits only for time zero, the above indicated post-reflood time, and the transition time.

The major edit at 40.5 seconds is close to the time of peak pressure. The major edit at 50.5 seconds is close to the end-of-blowdown time. The major edit at 125 seconds is close to the end-of-reflood time.

CLPD LOCA Containment Response FSAR Case

Time (sec)	Event
0.0	Break opens
24	Time of peak pressure
25.148	End-of-blowdown
47	End of reflood
4000	Post-reflood time, previously selected for containment energy balance determination
9000	RELAP5 to GOTHIC transition time

The RELAP5 major edits that are available in the computer run output for this case, at or close to the above times, are as follows:

1 0 seconds
2) 20.5 seconds
3) 30.5 seconds
4) 50.5 seconds
4) 4000 seconds
5) 9000 seconds

As shown above, there is an exact match between the sequence of events times and major edits only for time zero, the above indicated post reflood time, and the transition time. The major edits at 20.5 seconds and at 30.5 seconds bracket the time of peak pressure and the end-of-blowdown time. The major edit at 50.5 seconds is close to the end-of-reflood time.

Approach to Calculating Temperature History

The manipulation of the major edits to obtain the desired temperature history information is based on characterizing the structure stored energy and the wall film conditions in the RCS and SG at any given time, according to the following simple equations, if one assumes heat transfer to single phase fluid:

$$Q_{SE} = (\rho C_p)V(T_{avg} - 32)$$

$\dot{Q}_{film} = h_{film}A(T_w - T_{fluid})$, where

ρC_p are metal physical properties determined from data given in the RELAP5 inputs. These inputs were fitted into polynomials as a function of temperature to enable calculating local physical properties.

V and A are obtained from the structure geometry inputs. The elements for determining these parameters are extracted from the RELAP5 inputs and tabulated. The geometric inputs tabulated are: (1) inner and outer radii for cylindrical geometry along with total length, (2) thickness and surface area for rectangular geometry, and (3) inner and outer radii and spherical fraction for spherical geometry.

T_{avg} , the average slab temperature, is extracted and tabulated; it is given in RELAP5 major edits as heat structure volume average temperature.

T_w , the wall temperature, is extracted and tabulated; it is given in RELAP5 major edits as left side and right side heat structure surface temperatures.

h_{film} , the film heat transfer coefficient, is extracted and tabulated; it is given in RELAP5 major edits as left side and right side heat structure film heat transfer coefficients.

T_{fluid} , the fluid temperature, is extracted and tabulated; it is given in RELAP5 major edits for two-phase conditions as liquid and steam temperatures.

Temperature History Data Listings

The tabular listings of temperature history information (non-proprietary) are described below and are provided in the compact disk enclosed with the transmittal letter (NRC:09:060 dated May 22, 2009) accompanying this response.

RCS and SG Metal Geometries

The RCS and SG metal geometries are provided in Tables 1 and 2, respectively.

Temperature History Information at Time Zero

The temperature history information at time zero is tabulated only once because all the LOCA cases are initialized to the same initial plant operating conditions. The RCS information is provided in Tables (stored energy), Table 4 (wall film conditions), and Table 5 (fluid conditions). The SG information is provided in Table 6 (stored energy), Table 7 (wall film conditions), and Table 8 (fluid conditions).

Temperature History Information for HL LOCA FSAR Case

Temperature History Information at Time 20 Seconds

The RCS information is provided in Table HLt1-1 (stored energy), Table HLt1-2 (wall film conditions), and Table HLt1-3 (fluid conditions). The SG information is provided in Table HLt1-4 (stored energy), Table HLt1-5 (wall film conditions), and Table HLt1-6 (fluid conditions).

Temperature History Information at Time 30 Seconds

The RCS information is provided in Table HLt2-1 (stored energy), Table HLt2-2 (wall film conditions), and Table HLt2-3 (fluid conditions). The SG information is provided in Table HLt2-4 (stored energy), Table HLt2-5 (wall film conditions), and Table HLt2-6 (fluid conditions).

Temperature History Information at Time 3957 Seconds

The RCS information is provided in Table HLt3-1 (stored energy), Table HLt3-2 (wall film conditions), and Table HLt3-3 (fluid conditions). The SG information is provided in Table HLt3-4 (stored energy), Table HLt3-5 (wall film conditions), and Table HLt3-6 (fluid conditions).

Temperature History Information at Time 5470 Seconds

The RCS information is provided in Table HLt4-1 (stored energy), Table HLt4-2 (wall film conditions), and Table HLt4-3 (fluid conditions). The SG information is provided in Table HLt4-4 (stored energy), Table HLt4-5 (wall film conditions), and Table HLt4-6 (fluid conditions).

Temperature History Information for CLPS LOCA FSAR Case

Temperature History Information at Time 40.5 Seconds

The RCS information is provided in Table CLSt1-1 (stored energy), Table CLSt1-2 (wall film conditions), and Table CLSt1-3 (fluid conditions). The SG information is provided in Table CLSt1-4 (stored energy), Table CLSt1-5 (wall film conditions), and Table CLSt1-6 (fluid conditions).

Temperature History Information at Time 50.5 Seconds

The RCS information is provided in Table CLSt2-1 (stored energy), Table CLSt2-2 (wall film conditions), and Table CLSt2-3 (fluid conditions). The SG information is provided in Table CLSt2-4 (stored energy), Table CLSt2-5 (wall film conditions), and Table CLSt2-6 (fluid conditions).

Temperature History Information at Time 125 Seconds

The RCS information is provided in Table CLSt3-1 (stored energy), Table CLSt3-2 (wall film conditions), and Table CLSt3-3 (fluid conditions). The SG information is provided in Table CLSt3-4 (stored energy), Table CLSt3-5 (wall film conditions), and Table CLSt3-6 (fluid conditions).

Temperature History Information at Time 4000 Seconds

The RCS information is provided in Table CLSt4-1 (stored energy), Table CLSt4-2 (wall film conditions), and Table CLSt4-3 (fluid conditions). The SG information is provided in Table CLSt4-4 (stored energy), Table CLSt4-5 (wall film conditions), and Table CLSt4-6 (fluid conditions)

Temperature History Information at Time 10000 Seconds

The RCS information is provided in Table CLSt5-1 (stored energy), Table CLSt5-2 (wall film conditions), and Table CLSt5-3 (fluid conditions). The SG information is provided in Table CLSt5-4 (stored energy), Table CLSt5-5 (wall film conditions), and Table CLSt5-6 (fluid conditions).

Temperature History Information for CLPD LOCA FSAR Case

Temperature History Information at Time 20.5 Seconds

The RCS information is provided in Table CLDt1-1 (stored energy), Table CLDt1-2 (wall film conditions), and Table CLDt1-3 (fluid conditions). The SG information is provided in Table CLDt1-4 (stored energy), Table CLDt1-5 (wall film conditions), and Table CLDt1-6 (fluid conditions).

Temperature History Information at Time 30.5 Seconds

The RCS information is provided in Table CLDt2-1 (stored energy), Table CLDt2-2 (wall film conditions), and Table CLDt2-3 (fluid conditions). The SG information is provided in Table CLDt2-4 (stored energy), Table CLDt2-5 (wall film conditions), and Table CLDt2-6 (fluid conditions).

Temperature History Information at Time 50.5 Seconds

The RCS information is provided in Table CLDt3-1 (stored energy), Table CLDt3-2 (wall film conditions), and Table CLDt3-3 (fluid conditions). The SG information is provided in Table CLDt3-4 (stored energy), Table CLDt3-5 (wall film conditions), and Table CLDt3-6 (fluid conditions).

Temperature History Information at Time 4000 Seconds

The RCS information is provided in Table CLDt4-1 (stored energy), Table CLDt4-2 (wall film conditions), and Table CLDt4-3 (fluid conditions). The SG information is provided in Table CLDt4-4 (stored energy), Table CLDt4-5 (wall film conditions), and Table CLDt4-6 (fluid conditions).

Temperature History Information at Time 9000 Seconds

The RCS information is provided in Table CLDt5-1 (stored energy), Table CLDt5-2 (wall film conditions), and Table CLDt5-3 (fluid conditions). The SG information is provided in Table CLDt5-4 (stored energy), Table CLDt5-5 (wall film conditions), and CLDt5-6 (fluid conditions).

h. The empirical models for steam condensation presented in the Midland FSAR are supported by test data from the 1/3 scale steam-water mixing test series. The models presented in Section 6.2.1.3.3.2-d of the Midland FSAR are not utilized for the U.S. EPR analysis. Instead, the interphase mass and heat transfer are calculated by RELAP5/MOD2-B&W. RELAP5/MOD2-B&W incorporates a two-fluid, non-equilibrium, non-homogeneous, hydrodynamic model for transient simulation of the two-phase system behavior. It has built-in models to calculate interphase drag, interphase mass, and heat transfer. RELAP5/MOD2-B&W has been benchmarked extensively to test data and used for analyzing numerous pressurized water reactors.

The most limiting scenario for the U.S. EPR is a pump suction break with two trains of ECCS available to inject to the intact loops. The condensation and mixing in the cold legs predicated by RELAP5/MOD2-B&W for this scenario has been compared to test data and the results are provided below.

Upstream of ECC injection nozzle, the thermodynamic ratio $R_T = \dfrac{W_{ECC} C_P (T_{SAT} - T_{ECC})}{W_{STM}(h_{STM} - h_f)}$ in the two intact loops with ECC injection is calculated to be 1.0 for the first 400 seconds, and 1.6 between 400 and 800 seconds. The condensation efficiency (defined as the ratio of the measured condensation rate to the condensation rate needed to heat the ECC to saturation) for the UPTF tests was found to be 80 – 100% when the thermodynamic ratio is less than 1.0. When the thermodynamic ratio is above 1.0 all the steam is condensed, as shown in Figure 06.02.01.03-1-3-5.

Figure 06.02.01.03-1-3-5—UPTF Integral and Separate Effects Cold Leg Injection Tests Results—Condensation (Stratified Flow Points) (from Figure 5-12 of Reference 1)

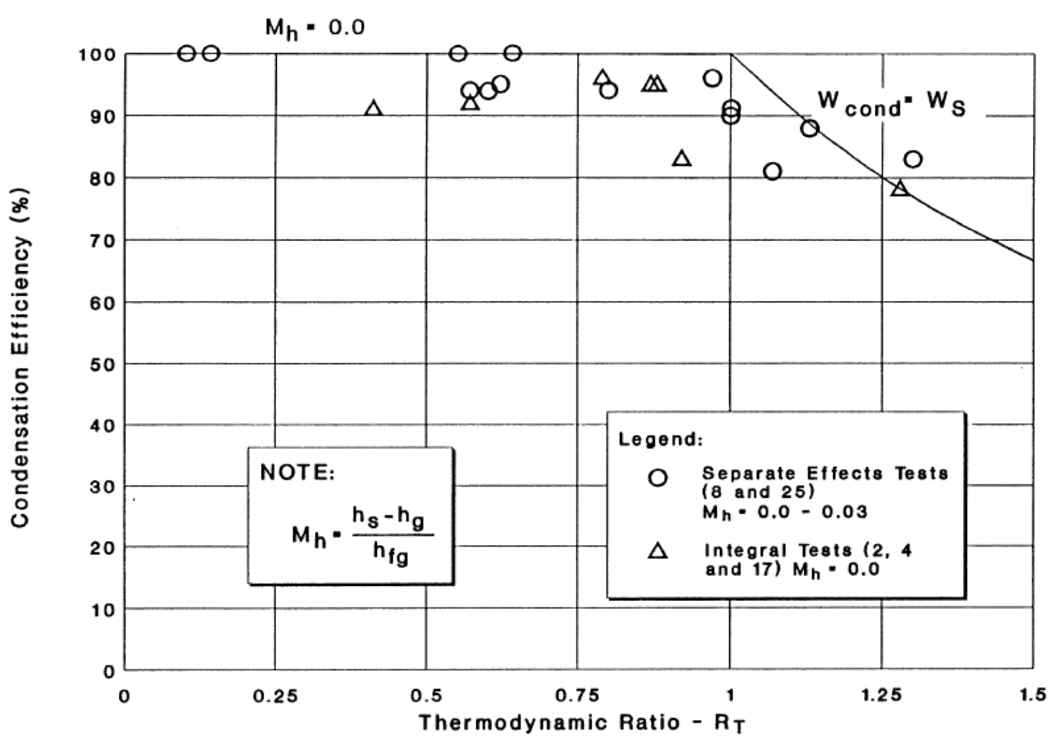

The EPRI 294-2 test data (Reference 2) show the ECC water at the downcomer inlet is about 5°F subcooled for a thermodynamic ratio of 1.0 and 50°F subcooled for a thermodynamic ratio of 1.6. In this range, the fact that more than 90% of the steam is condensed by ECC indicates strong condensation occurred in the cold legs.

Based on the above discussion, at least 80% of the steam is condensed in the cold legs with ECC injection. The uncondensed steam, along with the steam from the intact cold leg not receiving ECC injection, flows to the downcomer and out the broken cold leg. As the cold water enters the downcomer, mixing and condensation is very high when the nozzle belt area of the downcomer is voided.

RELAP5/MOD2-B&W predicts a very low steam condensation in the cold legs. The liquid temperature at the cold leg nozzles of intact loops with ECC injection is about 135°F, which is about 150°F subcooled (see Figure 06.02.01.03-1-3-6). The overall condensation in the cold legs predicted by RELAP5/MOD2-B&W is much lower comparing to the test data. The RELAP5/MOD2-B&W predicted condensation efficiency at the cold leg nozzles of intact loops with ECC injection is below 25%, while the test data show greater than 60% condensation efficiency in this range (see Figure 06.02.01.03-1-3-7).

As the steam and liquid reach the cold leg-to-downcomer junction, RELAP5/MOD2-B&W predicts very good mixing in the downcomer region. The liquid in the cold leg nozzle of the broken loop is about 25°F subcooled (see Figure 06.02.01.03-1-3). Upon leaving the downcomer, RELAP5/MOD2-B&W predicts condensation efficiency is below 90%, while the test data show nearly 100% condensation efficiency (see Figure 06.02.01.03-1-3); note the thermodynamic ratio at the cold leg nozzle of the broken loop for the U.S. EPR calculation is the average of all three intact loops).

As the steam and liquid leave the downcomer to the break, condensation occurs in the broken loop piping. Again, RELAP5/MOD2-B&W predicts little condensation in this piping region.

Additional mixing and condensation occur in the reactor coolant pump. RELAP5/MOD2-B&W predicts that the liquid is nearly saturated after leaving the pump. The amount of mixing and condensation occurring in the pump is realistic considering the effect of the pump's baffle and the change in flow direction within the pump. The liquid flowing out the break is close to saturation, which is supported by the test data.

References:

1. MPR-1208, "Summary of Results from the UPTF Cold Leg Flow Regime Separate Effects Tests, Comparison to Previous Scaled Tests and Application to U.S. Pressurized Water Reactors," MPR Associates, October 1992.

2. EPRI 294-2 Final Report, "Mixing of Emergency Core Cooling Water with Steam: 1/3-Scale Test and Summary," Electric Power Research Institute, June 1975.

Figure 06.02.01.03-1-3—ECCS Subcooling at DC Inlet versus Thermodynamic Ratio (EPRI 294-2 Data and Values Calculated for the U.S. EPR)

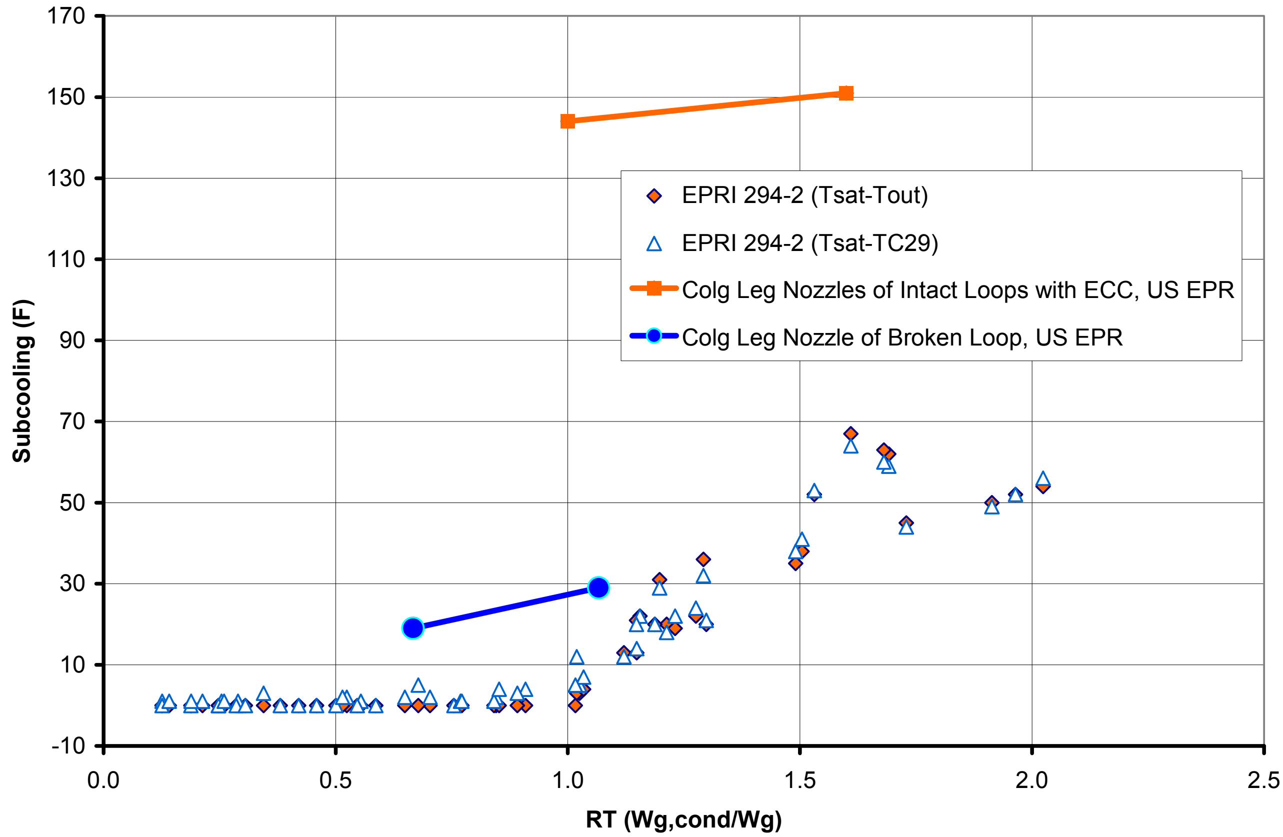

Figure 06.02.01.03-1-3—Condensation Efficiency versus Thermodynamic Ratio (EPRI 294-2 Data and Values Calculated for the U.S. EPR)

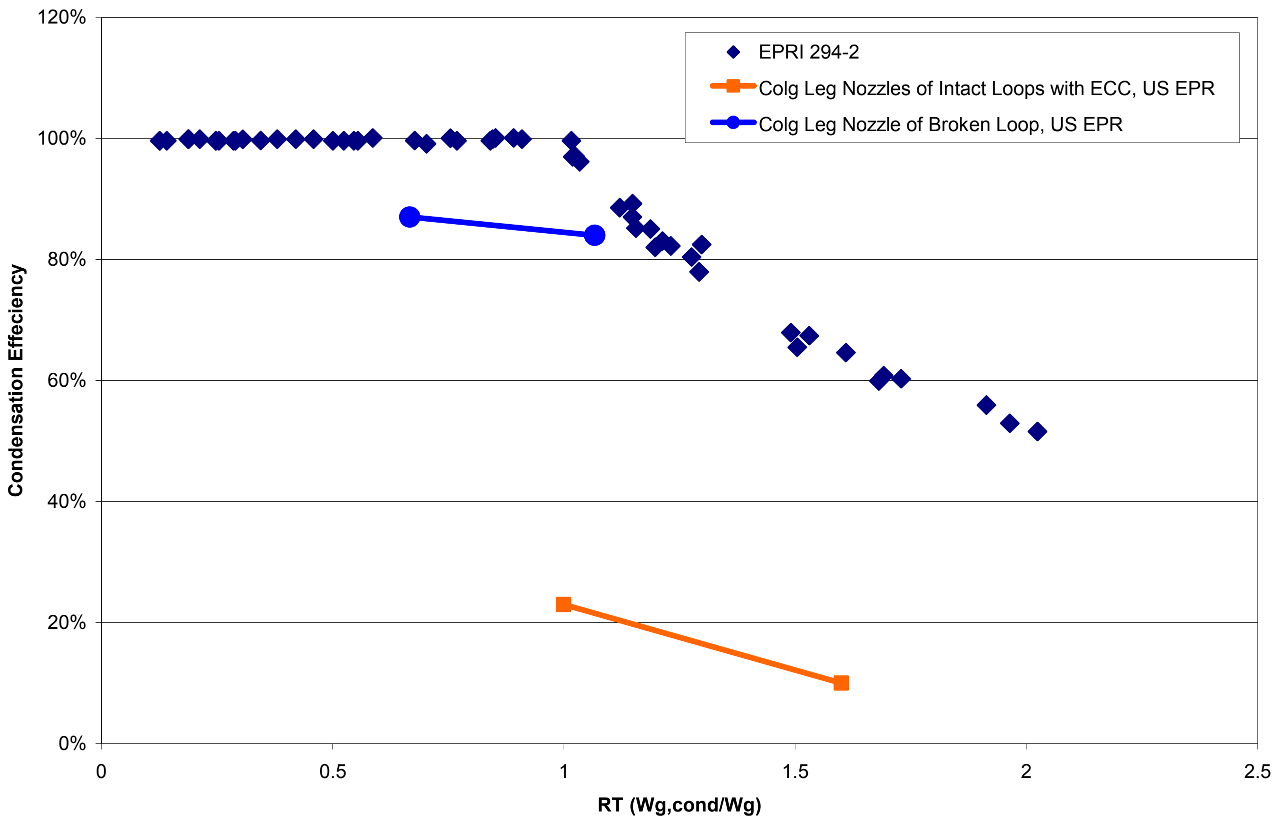

i. A response to this question was provided in AREVA NP Technical Report ANP-10299P.

j. A response to this question was provided in AREVA NP Technical Report ANP-10299P.

k. A response to this question was provided in AREVA NP Technical Report ANP-10299P.

l. A response to this question was provided in AREVA NP Technical Report ANP-10299P.

m. A response to this question was provided in AREVA NP Technical Report ANP-10299P.

n. A response to this question was provided in AREVA NP Technical Report ANP-10299P.

o. A response to this question was provided in AREVA NP Technical Report ANP-10299P.

p. A response to this question was provided in AREVA NP RAI 82 Response Supplement 1.

FSAR Impact:

The U.S. EPR FSAR will not be changed as a result of this question.

Question 06.02.01.04-1:

RAI - 6.2.1.4, Conservativeness of the Secondary System Break Mass and Energy Release Calculations (Relates to FSAR Section 6.2.1.4 and SRP Section 6.2.1.4)

a. Describe how energy stored in secondary system metal (steam generator vessel, tubing, tubesheets, steam line, feedwater line) was treated in the mass and energy release calculations. Describe the heat transfer models that were used and justify that they are conservative. Was nucleate boiling heat transfer used below the two phase level in the affected steam generator? If a different heat transfer model was used, justify that use of the model is conservative.

b. Identify the break discharge model (HEM, Moody, others) and discharge coefficient that was used for the main steam line break analysis and justify that the assumptions are conservative for containment analysis.

c. What decay heat model was used? [ ]

   Provide justification that the model is conservative for containment analysis.

d. From BAW-10169 which is referenced, it is understand that a stuck control rod assembly was assumed in the calculations. Verify that that was the case. The effect of a stuck control rod may be a return to power within the reactor core which may increase the energy available to be released to the containment. Show the effect of the stuck control rod on reactor power by providing a plot of reactor power for the limiting case and justify that the reactor power calculated by RELAP5 is conservative for MSLB mass and energy release calculations.

e. So that the NRC staff may perform additional confirmatory containment analyses provide mass and energy release data for the double ended steam line break cases with 20% and 80% power.

f. FSAR Section 6.2.1.4.1.2 states that during periods when liquid entrainment out of the break is predicted by RELAP5, that the energy of the fluid is set to saturated steam. Provide more detail of how this is done. Were code modifications made? If so, the modifications should be described and justified.

g. For the postulated double ended break of a steam line at 50% power provide the energy and mass content of the primary system metal and fluid and the secondary system metal and fluid at the beginning of the accident and at the end of the blowdown.

h. FSAR Section 6.2.1.4.3.3 states that the volume of water in the unisolated section of main feedwater piping is considered small and is not significant for containment analysis and therefore not considered. Provide additional justification such as comparing the unisolated feedwater mass to the total mass of the affected steam generator.

i. FSAR Table 6.2.1-22 which provides the mass and energy flow from the limiting main steam line break shows an initial flow of 7956 lbm/sec of steam which increases to 13691 lbm/sec at 5 seconds. Since steam pressure will be greatest at the beginning of the event, describe the mechanisms by which the calculated steam flow is lower at the beginning of the event and justify that this treatment is conservative.

j. FSAR Section 6.2.1.4.2 states that the RELAP5 code was used to determine the mass and energy released during the blowdown. If other methodology was used to determine the mass and energy release after the blowdown period, describe this methodology and justify that it is conservative for containment analysis.

k. Postulated feedwater Line Break Accidents were not addressed in FSAR Section 6.2.1.4. Provide evaluations of the containment consequences of postulated feedwater line break accidents.

l. FSAR Section 6.2.1.4.2 states that the RELAP5 code was used to determine the mass and energy released during the blowdown. Provide a diagram of the RELAP5 noding diagram and justify that it is appropriate for EPR MSLB analyses.

Response to Question 06.02.01.04-1:

a. A response to this question was provided in AREVA NP RAI 82 Response Supplement 1.

b. A response to this question was provided in AREVA NP's original response to RAI 82.

c. A response to this question was provided in AREVA NP's original response to RAI 82.

d. A response to this question was provided in AREVA NP RAI 82 Response Supplement 1.

e. A response to this question will be provided by June 23, 2009.

f. A response to this question was provided in AREVA NP's original response to RAI 82.

g. A response to this question will be provided by June 23, 2009.

h. A response to this question will be provided by June 23, 2009.

i. There are two reasons the initial steam flow is less than the steam flow at 5 seconds. First, the mass and energy release values that are input to GOTHIC are calculated from the integrated values from RELAP5/MOD2-B&W. Use of instantaneous values directly from RELAP5/MOD2-B&W would be limited to the resolution afforded by the frequency of minor edits in the RELAP5/MOD2-B&W run. Integrated values of mass and energy release are calculated at every calculation time step by RELAP5/MOD2-B&W, and therefore provide an accurate representation of the mass and energy release.

   A simple hand calculation is performed to convert the integrated values from RELAP5/MOD2-B&W into the average instantaneous values for input to GOTHIC. As a consequence of using integrated output, the integrated value calculated by RELAP5/MOD2-B&W at the start of the event is zero, and the maximum flow does not occur at the time of the break. The integrated values calculated by RELAP5/MOD2-B&W are preserved when they are input to GOTHIC as instantaneous values.

   Second, the entrained liquid release at the start of the event is nearly zero. As the transient progresses, large amounts of liquid can be entrained depending on the initial power level and the size of the break. All entrained liquid is treated as saturated steam by adding the entrained instantaneous liquid mass flow rate to the instantaneous steam mass flow rate in a RELAP5/MOD2-B&W control variable that is integrated to produce the total steam mass release. In this way, entrained liquid release is treated as steam release, and the liquid mass flow rate of entrained liquid is assigned the enthalpy of the steam release. For this reason, even though the RELAP5/MOD2-B&W junction that models the break experiences entrained liquid flow, U.S. EPR FSAR, Tier 2, Table 6.2.1-22 indicates that all releases are steam with no liquid release. A consequence of treating entrained liquid as steam is that the maximum steam flow rate occurs at approximately 5.0 seconds in the table.

j. The RELAP5/MOD2-B&W computer code is used to determine the mass and energy release during blowdown. All scenarios evaluating break size and initial power level credit operator action at 1800 seconds to isolate emergency feedwater flow. In all these cases, steam generator dome pressure reaches a minimum pressure plateau by approximately 800 seconds. The pressure plateau is maintained by the emergency feedwater that boils-off upon entering the steam generator.

k. A response to this question was provided in AREVA NP's original response to RAI 82.

l. A response to this question was provided in AREVA NP RAI 82 Response Supplement 1.

FSAR Impact:

The U.S. EPR FSAR will not be changed as a result of this question.

Question 06.02.01.05-1:

a. Instead of the conservative heat transfer coefficients recommended by BTP 6-2 the minimum containment pressure analysis for the US-EPR realistic LOCA used heat transfer coefficients that were 1.7 times the Uchida correlation which were benchmarked against 1.0 times the Tagami correlation and then 1.2 times the Uchida correlation. These were described as best estimate. Provide: 1. Justification that the heat transfer correlations selected for the EPR minimum containment pressure analysis are indeed best estimate and 2. Provide the basis for the uncertainty in these coefficients so that these uncertainties may be applied in the realistic LOCA calculations.

b. FSAR Section 6.2.1.5.2 states that inside the containment, the IRWST water temperature is expected to be at the containment temperature of approximately 60°F, but could range as high as 120°F, which is the Technical Specification maximum value. The realistic large break LOCA methodology uses the value of 120°F for the minimum containment pressure calculation. Provide justification for the apparently non-conservative value selected for IRWST temperature.

c. According to FSAR Tier 2, Section 6.2.1.5.3, the passive heat sinks and thermo-physical properties were derived in accordance with Branch Technical Position 6-2, “Minimum Containment Pressure Model for PWR ECCS Performance Evaluation.” The BTP states that the data on passive heat sinks was compiled from previous reviews and used as a basis for the simplified model which it contains. This simplified model is stated to be acceptable for minimum containment pressure analyses for construction permit applications until a complete identification of available heat sinks can be made. Table 6.2.1.5 of FSAR Tier 2 (Containment heat sink inventory), shows the heat sink components, including their material, thickness and areas for EPR in detail. The staff further understands that the heat sink inventory for EPR is greater than that of operating plants. To demonstrate that the BTP containment heat sink inventory is conservative for EPR minimum containment pressure analysis, provide the results of a sensitivity study of the minimum containment pressure for which the heat sinks of Table 6.2.1.5 are used in place of those in the BTP.

d. Provide an evaluation of the effect of containment atmosphere leakage though containment openings before isolation including equipment and personnel hatches. What would be the effect of such leakage on the minimum calculated containment pressure calculation?

e. The staff understands that a realistic model as discussed in 10 CFR 50.46(a)(1)(i) is used to evaluate ECCS performance for EPR and that this model is used to provide the mass and energy release for the minimum containment pressure analysis. Section 6.2.1.5.1 of the FSAR states that the mathematical model that calculate the mass and energy releases to the containment for the minimum containment pressure analysis conforms the requirements for deterministic ECCS evaluation models in 10 CFR Part 50, Appendix K. Clarify if the model to calculate the mass and energy release is realistic as discussed in 10 CFR 50.46(a)(1)(i) or if the model is an follows Appendix K to 10CFR50 as prescribed in 10 CFR 50.46(a)(1)(ii).

f. Regulatory Guide 1.206 C.I.6.2.1.5(1) requests that for the minimum containment pressure analysis that applicants provide for the most severe break, the mass and energy release data used for the minimum containment pressure analysis. The mass and energy of safety injection fluid that is assumed to spill from the break directly to the containment floor should be included. The purpose this request is so that the staff may make independent containment pressure assessments. This information was provided in response to RAI 6.2.1-09a. The staff cannot use the mass and energy release data in a containment analysis computer code since the nitrogen accumulator gas release is lumped with the steam and water. Provide separate tables one containing the steam and water and the other containing the nitrogen release. Provide justification that input to the ICECON model in S-RELAP5 is properly accounting for the separate entry of steam and water as well as nitrogen.

g. The given initial pressure for the minimum containment pressure analysis is the normal atmospheric pressure. The initial temperatures inside and outside of the containment are lower than normally expected temperatures; thus, the initial condition appears to be conservative. However, it is not clear how the cold outside temperature was taken into account in the analyses. For instance, what initial temperature distribution through the containment wall was used? In addition, it is not clear whether the initial values have been varied and what range of variation was assumed for realistic LOCA. Provide this information.

h. Minimum containment pressure is calculated by the ICECON module embedded in S-RELAP5. Provide a noding diagram of the ICECON containment model and justify that the noding is conservative for calculating minimum containment pressure. In a presentation to the NRC staff January 29, 2008, Areva presented a sensitivity study showing that a multi-node GOTHIC model of the EPR produced containment pressure several psi lower than the single node model. Perform a similar noding sensitivity study using ICECON to show that noding detail is being conservatively accounted for.

Response to Question 06.02.01.05-1:

a. A response to this question will be provided by June 12, 2009.

b. **IRWST Water Temperature**

The realistic large break loss of coolant accident (RLBLOCA) model described in AREVA NP Document EMF-2103(P)(A), Revision 0, “Realistic Large Break LOCA Methodology for Pressurized Water Reactors,” April 2003, was used for the U.S. EPR RLBLOCA analysis. This approved methodology applies the sampled value of the containment temperature to the accumulators and the containment vapor and liquid, including the liquid in the in-containment refueling water storage tank (IRWST). ANP-10278P, Rev. 0, “U.S. EPR Realistic Large Break Loss of Coolant Accident Topical Report,” describes and demonstrates the applicability of EMF-2103(P)(A), Rev. 0 to the U.S. EPR.

In the current U.S. EPR FSAR RLBLOCA analysis, the containment temperature is sampled uniformly from a lower bound of 59°F to an upper bound of 122°F. This range corresponds to the Technical Specification Surveillance Requirements (SR) 3.5.4.1 for the IRWST.

The U.S. EPR FSAR, Tier 2, Section 6.2.1.5.2 will be changed to reflect this temperature range.

U.S. EPR RLBLOCA analyses sample containment temperature uniformly from a lower bound of 59°F to an upper bound of 131°F. This range corresponds to the Technical Specification limiting condition for operation (LCO) 3.6.5 containment air temperature. Sensitivity studies showed that using 131°F as the upper bound of the sampling range provides a slightly higher, thus conservative, peak cladding temperature result.

c. **Heat Sink Inventory**

The development of the heat sinks in the ICECON model begins with the heat structure groups in the U.S. EPR GOTHIC containment model. The GOTHIC containment model is based on a comprehensive listing of containment heat sinks. The following points pertain to the ICECON model used to perform the requested sensitivity study to demonstrate that the BTP containment heat sink inventory is conservative for U.S. EPR minimum containment pressure analysis.

1. The ICECON model treats the containment walls and the IRWST walls as two-sided heat structures. The IRWST walls are in contact with water on one side and the containment atmosphere on the other. The containment walls are in contact with the containment annulus on one side and the containment atmosphere on the other.

2. The ICECON model considers an increase in the surface area of un-insulated systems and components. The surface area of this additional heat sink is determined so that the total exposed internal steel heat sink area in ICECON is consistent with the total internal steel heat sink area recommended in Figure 1 of NUREG 0800 Branch Technical Position (BTP) 6-2. The combined containment volume (nominal containment gas volume plus nominal IRWST water volume) is 81,777 m^3 (2,887,927 ft^3). In accordance with Figure 1 of BTP 6-2, the total internal steel heat sink area is 3.5×10^4 m^2 (376,737 ft^2). It is assumed that the containment free volume in Figure 1 of BTP 6-2 ranges from 0.0 m^3 to 1.2×10^5 m^3.

3. All of the nominal heat transfer surface areas in the ICECON model are increased by 10% to increase the energy removed from the containment atmosphere.

The material properties of steel and concrete are consistent with BTP 6-2, Table 2. The paint layer is assumed to have the material properties of steel. The liner is modeled as being in contact with the concrete. That is, the air gap between the liner and concrete is neglected. The objective of these assumptions is to eliminate any insulating effects on the exposed surfaces of the heat structures.

A sensitivity study was performed using an ICECON model to assess the sensitivity of the containment pressure calculation to heat transfer surface area for three cases. The first case uses heat transfer surface areas corresponding to those in the U.S. EPR GOTHIC calculation. The second case incorporates Changes 1 and 2 above. The third case applies the 10% conservatism, Point 3 above, in addition to Points 1 and 2.

Figure 06.02.01.05c-1 compares the containment pressure for each case and shows that the ICECON model that applies a 1.1 surface area multiplier (Point 3) to the containment heat sink inventory incorporating BTP 6-2 assumptions (Points 1 and 2) calculates the lowest containment pressure.

Figure 06.02.01.05c-1—Containment Pressure Comparison

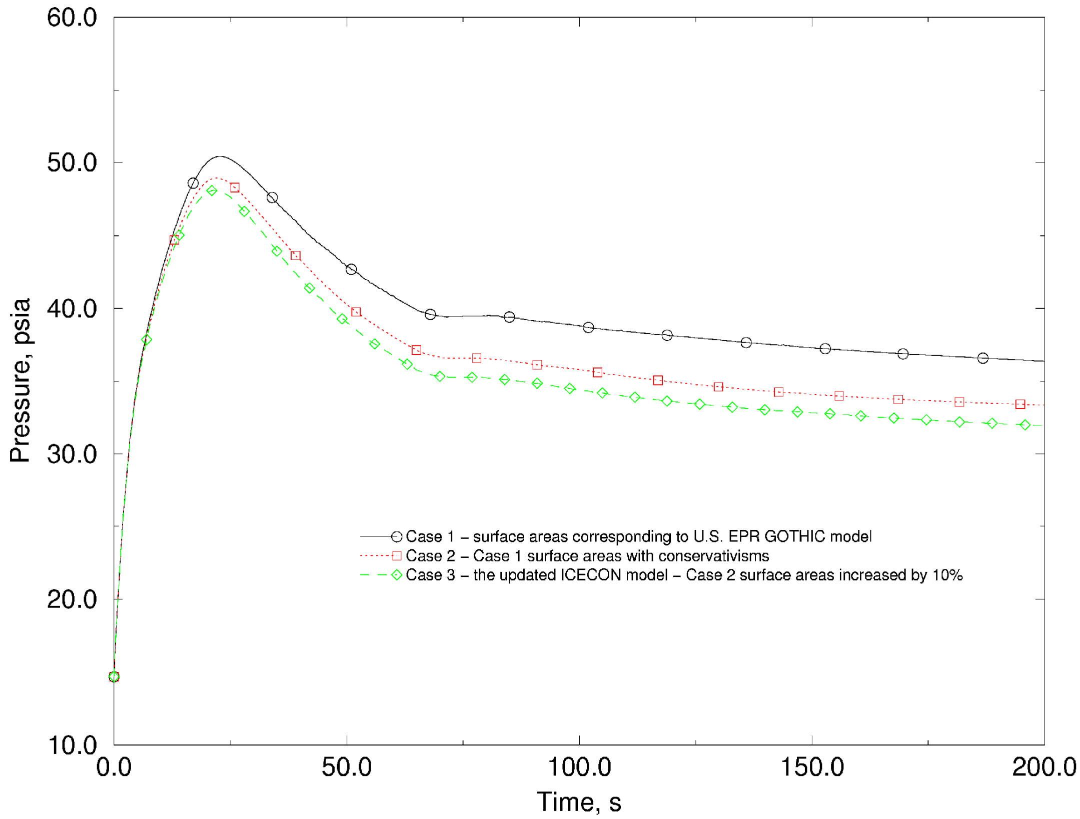

d. **Containment Leakage**

The ICECON model used in the U.S. EPR realistic large break loss of coolant accident (RLBLOCA) assessment does not consider containment leakage. This approach is consistent with the ICECON model that supports ANP-2695P, Revision 0, “Sequoyah Nuclear Plant Unit 1 Realistic Large Break LOCA Analysis.”

Containment Annulus In-Leakage

AREVA NP performed a sensitivity study to assess the effects of containment leakage on containment pressure calculations. Primary containment leakage at the maximum containment design pressure and temperature of 76.696 psia and 338°F is 9.8 cfm. The containment leakage is not isolated to conservatively increase the effect of containment leakage on the containment pressure calculation.

Figure 06.02.01.05d-1 shows no discernible effect on the containment pressure response.

Figure 06.02.01.05d-2 shows the containment is registering the leakage but it is very small (≈60 lbm/hr at its maximum). Figure 06.02.01.05d-3. shows only a very small amount of energy removed from the containment due to the leak.

A containment leakage curve was generated and then calibrated using the annulus in-leakage from primary containment during a LOCA at maximum containment pressure and temperature. Based on this curve, the containment leakage has no significant effect on the containment pressure calculation. Therefore, annulus in-leakage is not modeled in the RLBLOCA analysis.

Leakage Through Larger Openings

The containment purge subsystem contains the low airflow (partial purge) loop (KLA 1-2, which is used during outages, and prior to containment entry) and the high airflow (full purge) loop (KLA 3-4, which is used during outages). Of the valves in these loops, only the 20 in KLA 1-2 have the potential to be open for an RLBLOCA.

To calculate the RLBLOCA minimum containment pressure, the code uses ICECON to model the containment (EMF-CC-039(P), Revision 4, “ICECON: A Computer Program Used to Calculate Containment Back Pressure for LOCA Analysis (Including Ice Condenser Plants),” December 2007). ICECON, based on CONTEMPT 22, cannot model a leak that is isolated during the transient.

A GOTHIC model is modified to assess the effect of this leak on containment pressure. The reference GOTHIC model is based on a benchmark of ICECON to an equivalent GOTHIC model of the U.S. EPR containment for the first few minutes following a large break LOCA. In the benchmark, the integrated mass and energy release (MER) from S-RELAP5 is used to create the average mass flow rate and enthalpy input to both GOTHIC and ICECON. The modified GOTHIC model incorporates the purge valves, which could be open before shutdown, or containment penetrations during operation.

Figure 06.02.01.05d-4. shows a flowrate through the openings that drops to zero when the valves are shut 10 seconds after the containment pressure reaches the high containment pressure trip setpoint (four psig with 0.5 psi uncertainty). After a 0.5 second delay from the trip signal, the valves are required to close in five seconds or less. For this analysis, however, the time from the trip signal to the valves being fully closed is conservatively set to 10 seconds.

Figure 06.02.01.05d-5. compares the GOTHIC containment pressure prediction with leakage to the GOTHIC and ICECON predictions without leakage. From the GOTHIC results, modeling leakage through the larger openings produces a decrease of approximately 0.5 psi in containment pressure. An evaluation of the effect of this pressure decrease on peak cladding temperature (PCT) is provided below.

Sensitivity of Peak Cladding Temperature to Containment Back-Pressure

The following sensitivity study calculates a maximum and minimum containment pressure based on the variation in containment volume and temperature. That is, this sensitivity study demonstrates the difference between the maximum and minimum containment back-pressure responses, which are functions of the sampled containment volume and temperature. In addition, this sensitivity study relates this difference in containment pressure response to a difference in calculated PCT.

The study uses two cases. The first, Case 44, reports the highest PCT for the equilibrium cycle RLBLOCA analysis, as shown in U.S. EPR FSAR, Tier 2, Table 15.6-11. Case 44 has a PCT that occurs early in the transient. The second case, Case 18, is also from the equilibrium cycle RLBLOCA analysis, but has a PCT that occurs later in the transient. The study uses the S-RELAP5 transient input files associated with these two cases.

Consistent with Section 4.2.5 of EMF-2103, Revision 0, “Realistic Large Break LOCA Methodology for Pressurized Water Reactors,” August 2001, the containment volume is varied from the best-estimate value to the maximum possible free volume. In the sensitivity study, the containment volume is sampled uniformly from 2,887,927 ft^3 to 3,933,665 ft^3. The containment temperature is sampled uniformly from 59°F to 131°F.

Figure 06.02.01.05d-6. compares the containment pressure predictions for three cases using the S-RELAP5 transient input file for Case 44. The case with maximum containment volume and minimum containment temperature produces the lowest containment pressure and is approximately 5 psi lower than the base case for most of the transient. The peak cladding temperature in Figure 06.02.01.05d-7. reflects these differences in containment pressure calculations.

Figure 06.02.01.05d-8. compares the containment pressure prediction for two cases using the S-RELAP5 transient input file for Case 18. As in Figure 06.02.01.05d-6., the case with maximum containment volume and minimum containment temperature produces the lowest containment pressure and is approximately 5 psi lower than the base case for most of the transient. Figure 06.02.01.05d-9. shows that the PCT calculation for the code runs that use the S-RELAP5 transient input file for Case 18 is more sensitive to the difference in containment back-pressure.

A quantification of the change in PCT is presented in Table 06.02.02.05d-1. Case 44 with maximum containment volume and minimum containment temperature produces the highest PCT, a 35°F change from the base case. Although Case 18 experiences a 73°F increase in PCT using the maximum containment volume and minimum containment temperature, Case 44 still produces the highest PCT overall.

Thus, a small decrease in containment pressure, such as seen in Figure 06.02.01.05d-5. has only a small effect on the PCT calculation. Therefore, the leakage through the larger openings is not modeled in the RLBLOCA analysis.

Table 06.02.01.05d-1—Effect of Containment Pressure on Peak Cladding Temperature

		PCT (°F)	PCT Time (s)	ΔPCT (°F)
Case 44	Base	1436	35.1	-
	Max Vol, Min Temp	1471	40.3	35
	Best Est Vol, Max Temp	1433	35.8	-3
Case 18	Base	1395	60.4	-
	Max Vol, Min Temp	1468	123.8	73

Figure 06.02.01.05d-1—Containment Pressure Comparison

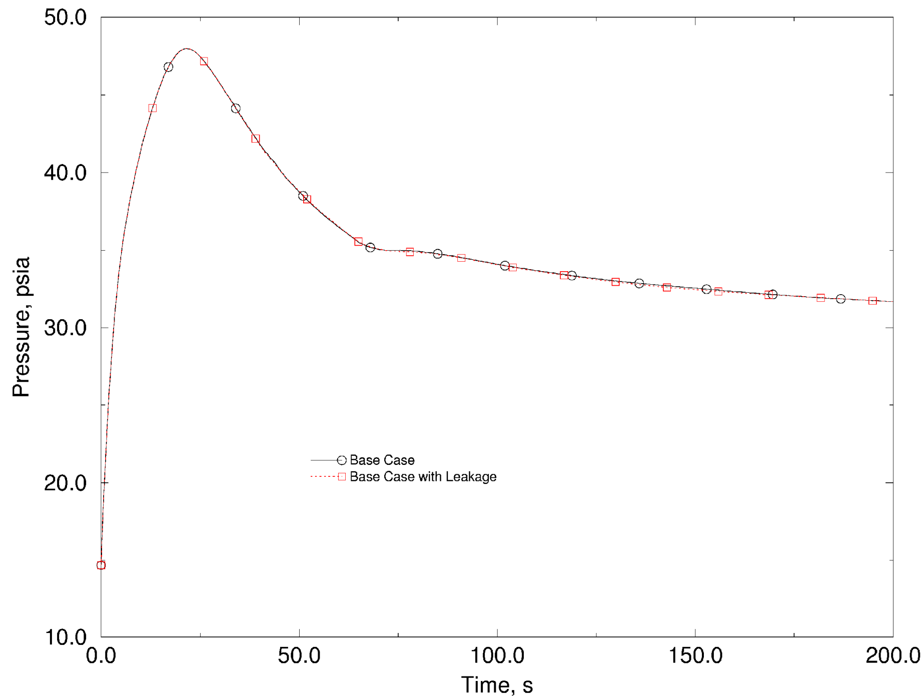

Figure 06.02.01.05d- 2.—Annulus In-Leakage Rate

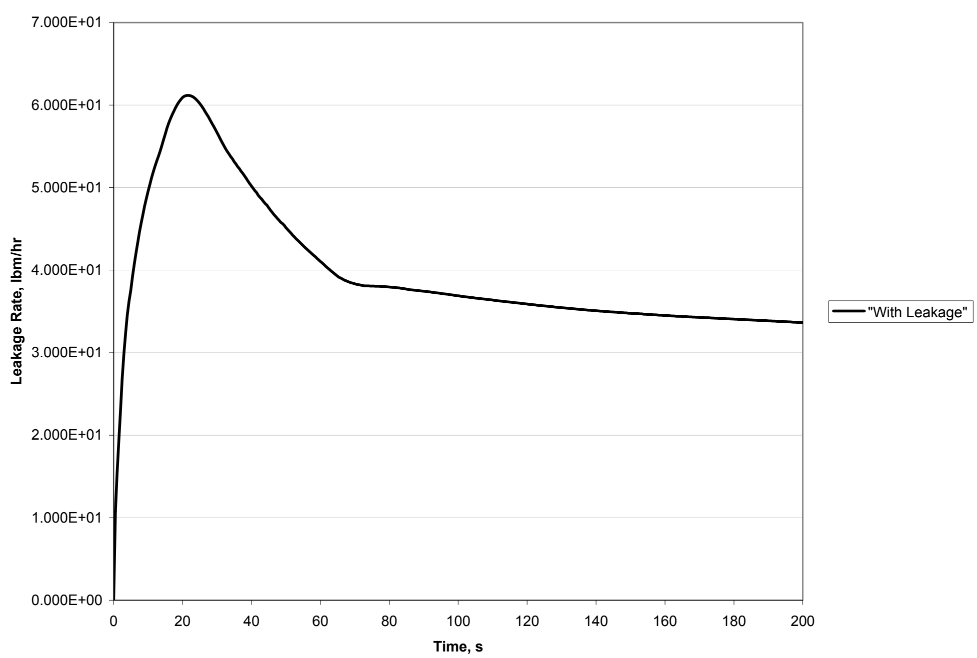

Figure 06.02.01.05d- 3.—Annulus In-Leakage Energy Gain

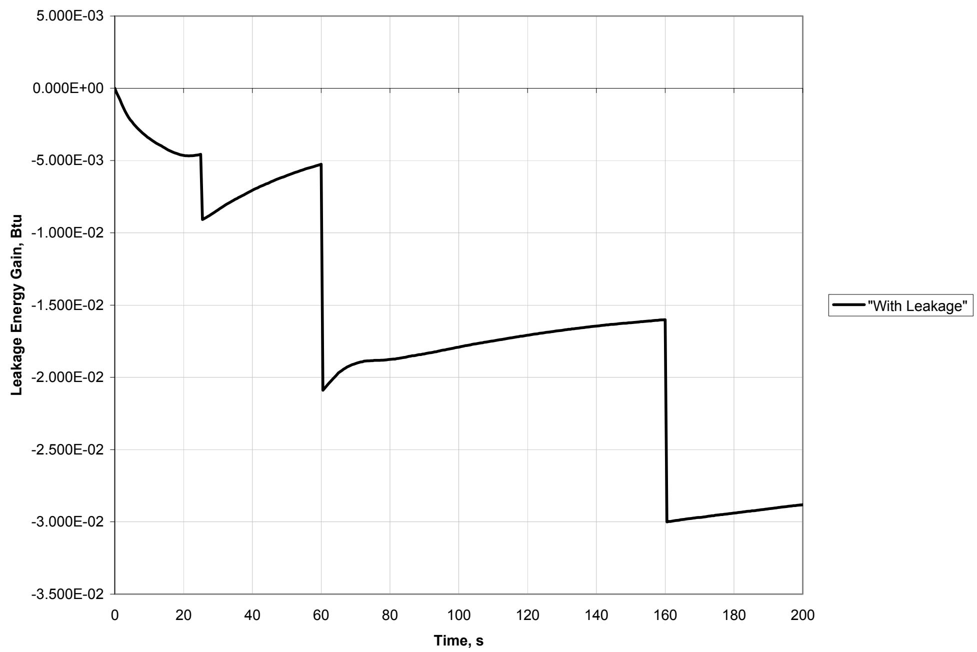

Figure 06.02.01.05d- 4.—Vapor and Liquid Drop Flowrates (Leakage through Large Openings)

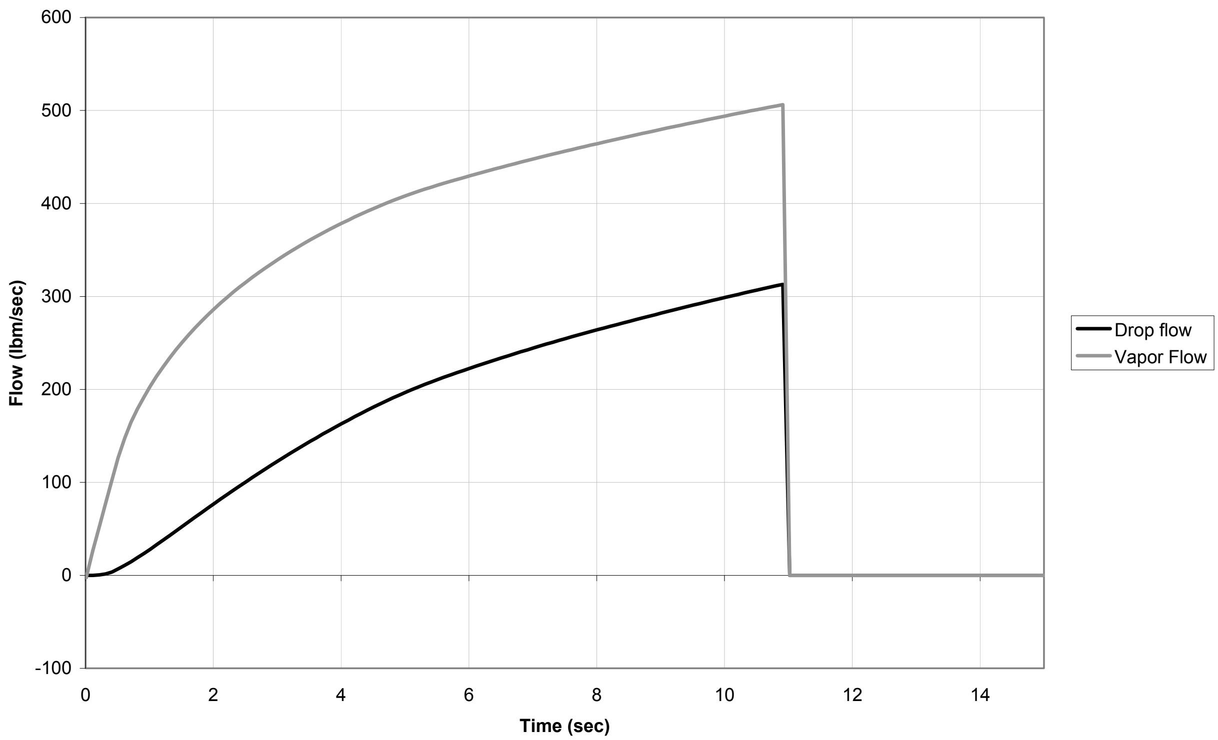

Figure 06.02.01.05d- 5.—Containment Pressure Comparison

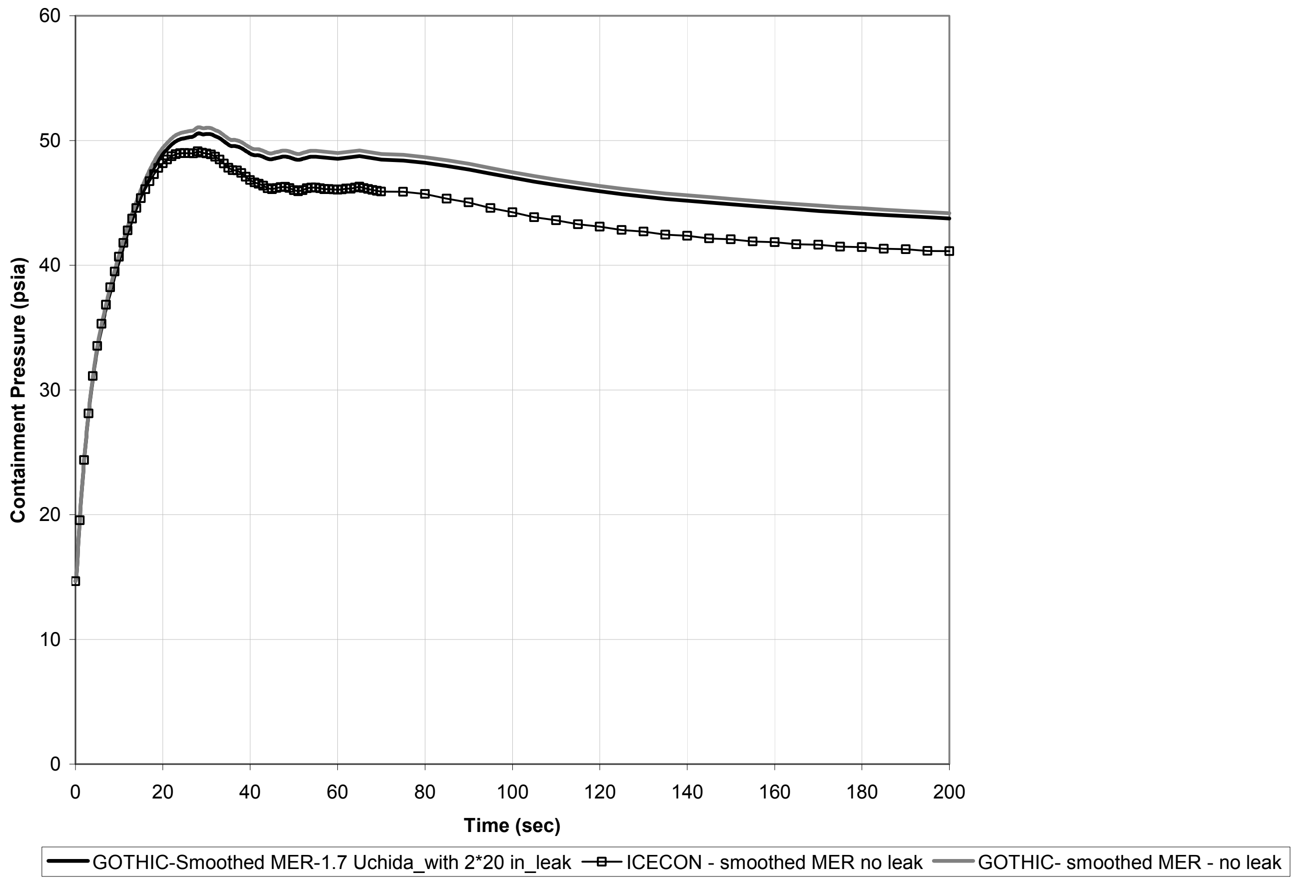

Figure 06.02.01.05d- 6.—Case 44 Containment Pressure Comparison

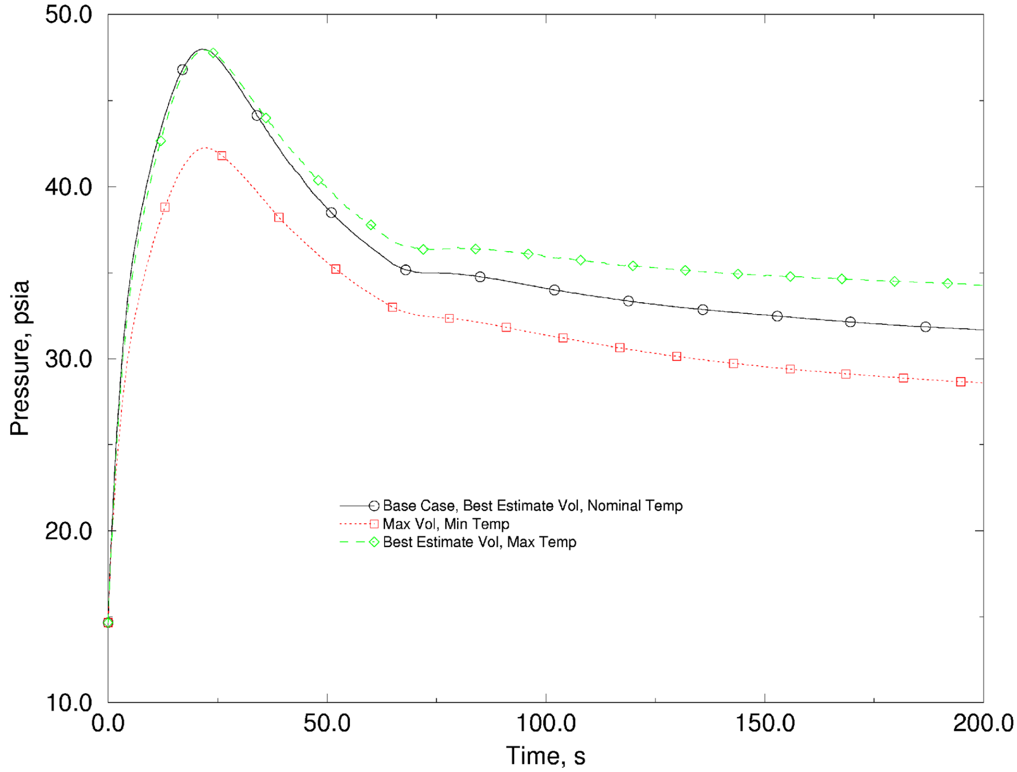

Figure 06.02.01.05d- 7.—Case 44 Peak Cladding Temperature Comparison

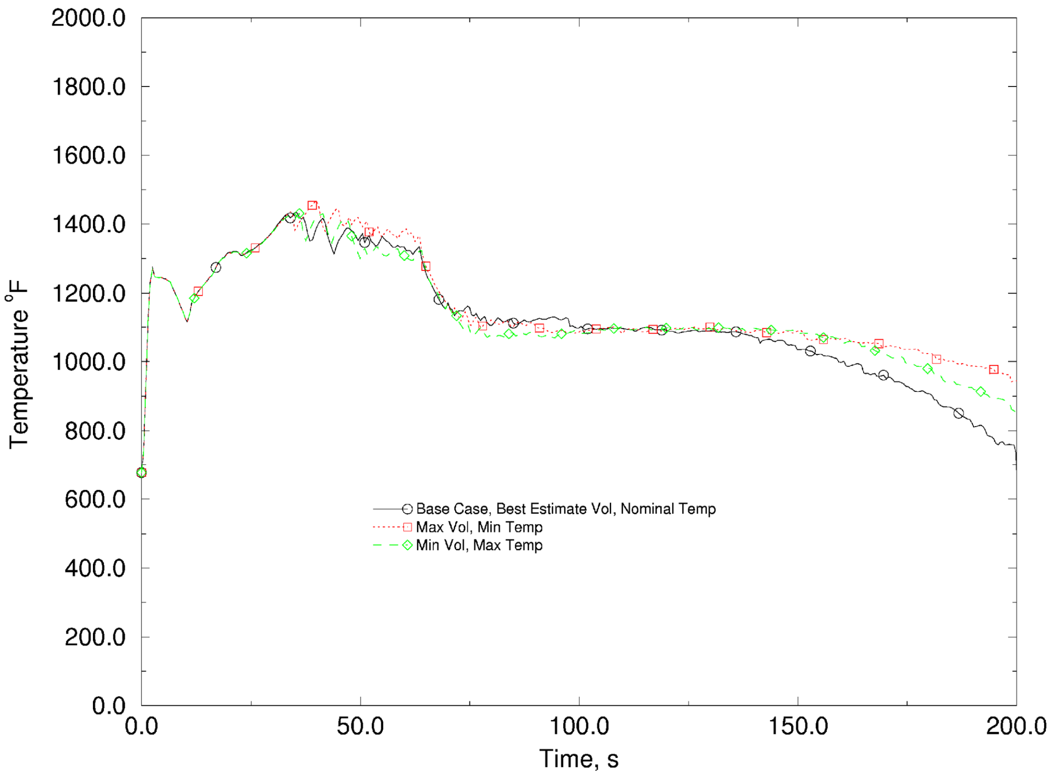

Figure 06.02.01.05d- 8.—Case 18 Containment Pressure Comparison

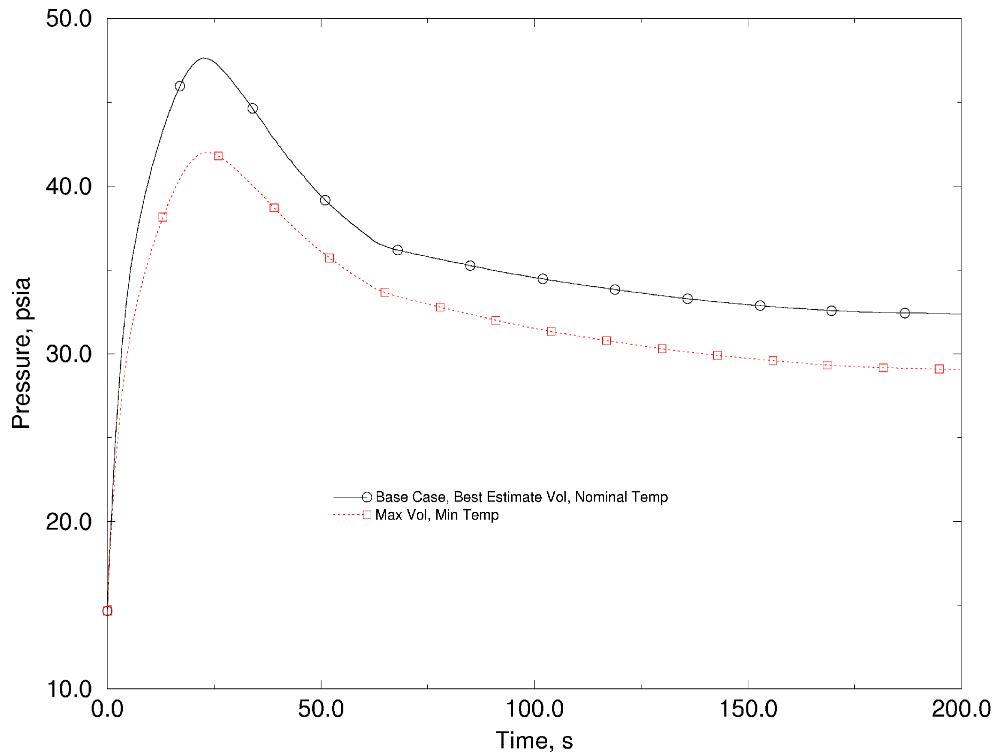

Figure 06.02.01.05d- 9.—Case 18 Peak Cladding Temperature Comparison

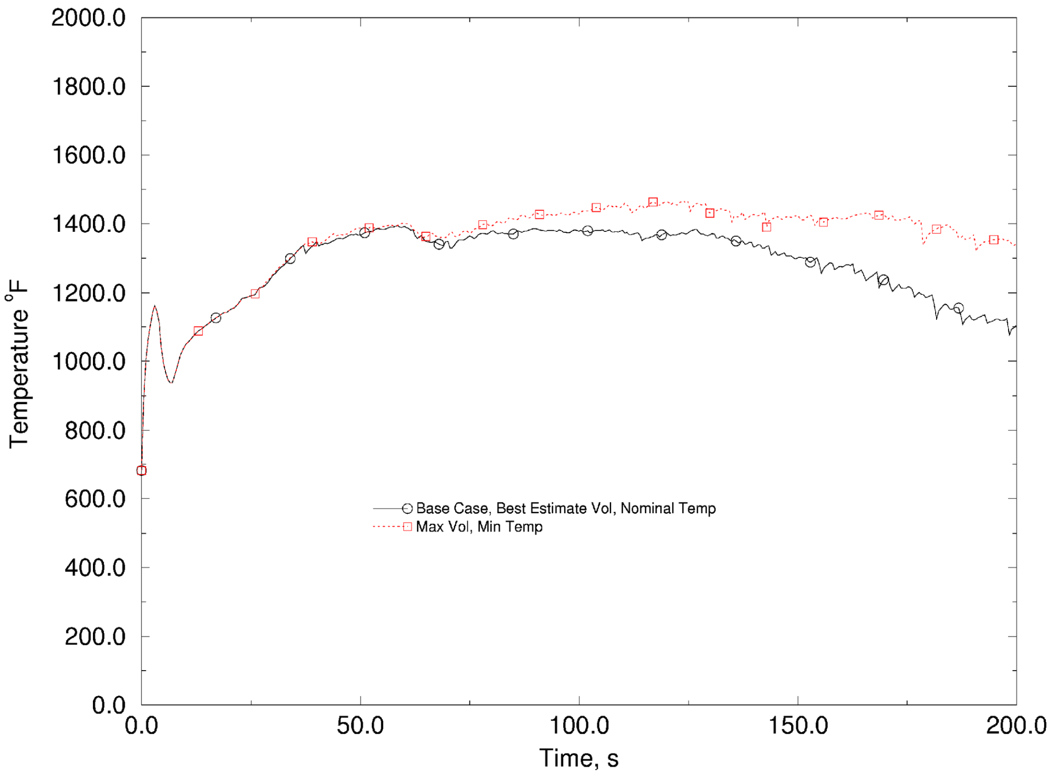

e. **Model Used to Evaluate ECCS Performance**

The model to calculate the mass and energy release is realistic, as discussed in 10 CFR 50.46(a)(1)(i).

U.S. EPR FSAR, Tier 2, Section 6.2.1.5.1 will be changed accordingly.

f. A response to this question will be provided by June 12, 2009.

g. **Annulus Conditions**

The ICECON model reported in U.S. EPR FSAR, Tier 2, Section 15.6 models the heat structures representing the containment walls and liner as being in contact with the containment atmosphere on one side. The other side, representing the boundary between the containment wall and the containment annulus, is treated as insulated. The ICECON model used in this response includes heat transfer to the containment annulus. This approach is consistent with ANP-2695P, Revision 0, “Sequoyah Nuclear Plant Unit 1 Realistic Large Break LOCA Analysis,” February 2008, Table 3-9, which describes the containment shell as being in contact with the containment annulus.

A sensitivity study comprised of three cases compares the sensitivity of the containment pressure calculation to the containment annulus boundary condition. The third case, the base case, models the annulus temperature at 45°F, which is the minimum winter design value. The heat transfer coefficient is set to 5.0 Btu/hr-ft^2-°F to be consistent with the analysis supporting ANP-2695P. The value of 5 Btu/hr-ft^2-°F is used for free convection in air and is the upper range of values for a free convection application (“Principles of Heat Transfer,” Frank Kreith, 3rd Edition, 1973, p.14).

The first case treats the boundary between the containment wall and the containment annulus as a symmetric boundary condition. The second case changes the temperature of the annulus to 20°F, which is consistent with the value used in the analysis of record.

Figure 06.02.02.05g-1 shows no discernible differences in containment pressure predictions due to annulus temperature conditions. An examination of Figure 06.02.02.05g-2 shows the temperature distributions through the containment wall. The temperatures at the inside of the containment wall are within approximately 1.5°F. Consequently, the effect of the heat transfer shown in Figure 06.02.02.05g-1 is indiscernible.

U.S. EPR RLBLOCA analyses will use an ICECON model that models the containment annulus at 45°F and uses a heat transfer coefficient of 5.0 Btu/hr-ft^2-°F for heat transfer to the containment annulus. The values of the annulus conditions are not varied during U.S. EPR RLBLOCA analyses.

Figure 06.02.01.05g-1—Containment Pressure Comparison

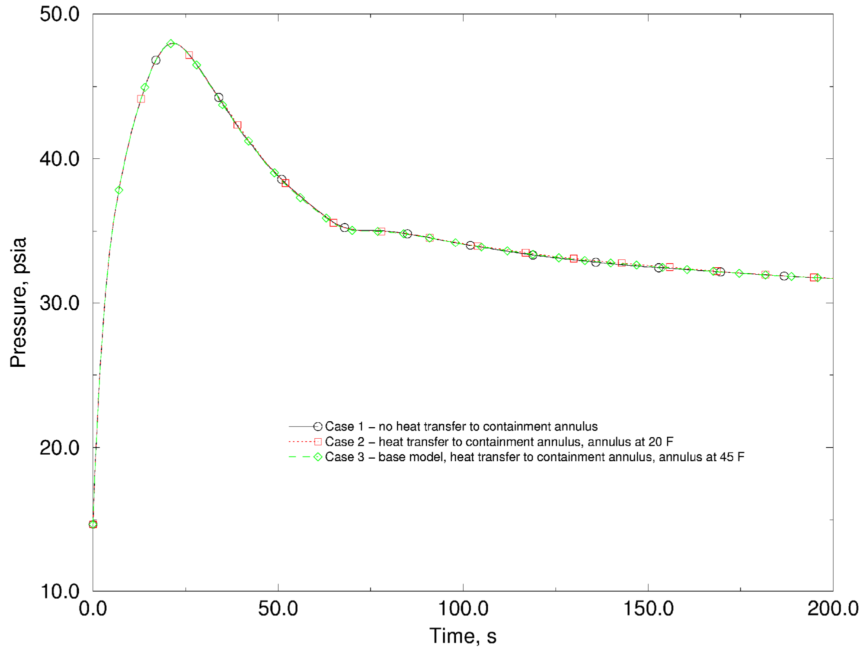

Figure 06.02.01.05g-2—Initial Containment Wall Mesh Point Temperatures

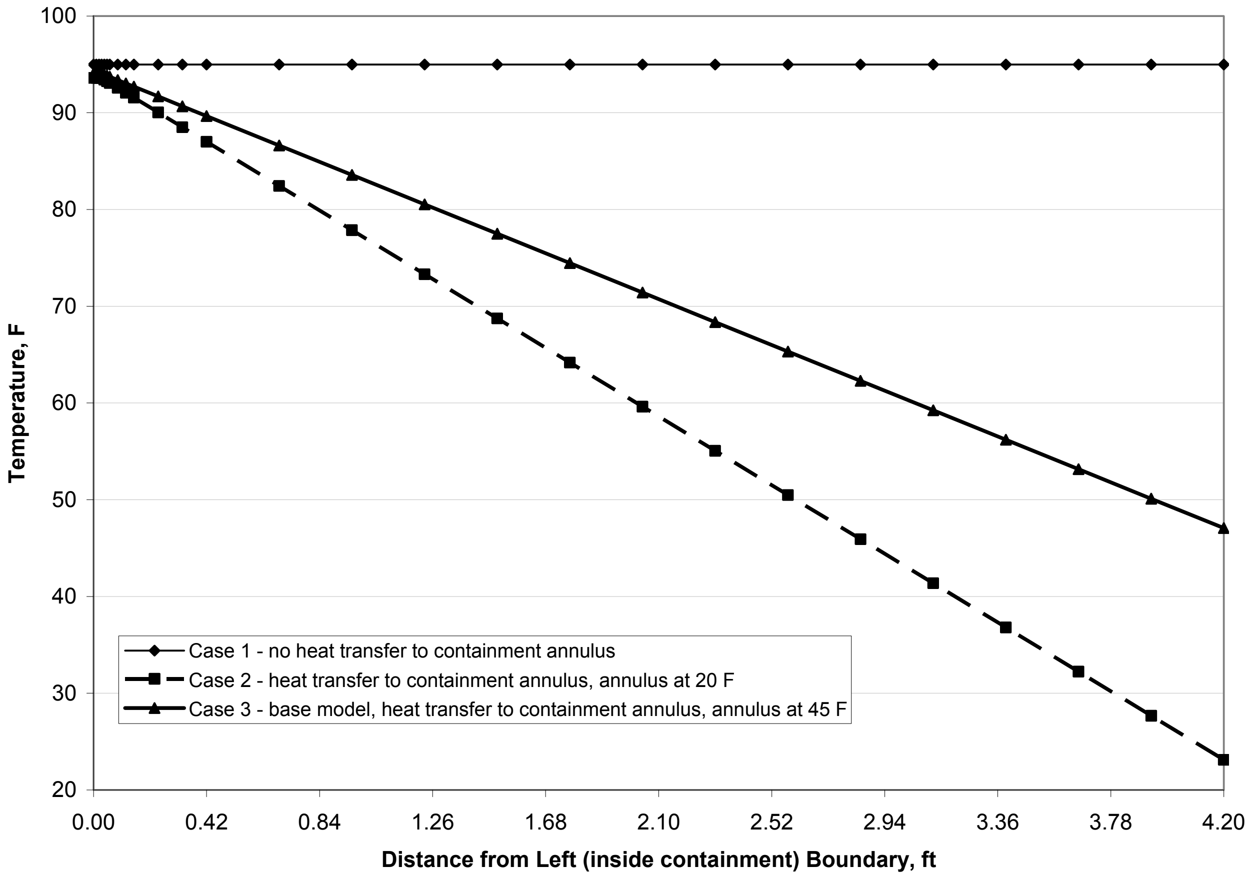

h. A response to this question will be provided by June 12, 2009.

FSAR Impact:

U.S. EPR FSAR, Tier 2, Section 6.2.1.5.1 will be revised as described in the response and indicated on the enclosed markup.

U.S. EPR FSAR, Tier 2, Section 6.2.1.5.2 will be revised as described in the response and indicated on the enclosed markup.

U.S. EPR Final Safety Analysis Report Markups

2.13 The RCB has a minimum containment free volume that is confirmed after construction.

2.14 The RCB and RB internal structures have a minimum containment heat sink surface area value.

06.02.01-12.c.3.2

3.0 Inspections, Tests, Analyses, and Acceptance Criteria

Table 2.1.1-8 lists the RB ITAAC.

Table 2.1.1-8—Reactor Building ITAAC (~~5~~ 6 Sheets)

	Commitment Wording	Inspections, Tests, Analyses	Acceptance Criteria
2.14	The RCB and RB internal structures have a minimum containment heat sink surface area value.	During construction, surface area dimensional deviations from the RCB and RB internal structures construction drawings will be analyzed for impact on the minimum containment heat sink surface area value.	As-built deviations to the surface area dimensions shown on construction drawings have been reconciled against the minimum value of 64,998 m^2 or 699,633 ft^2.

06.02.01-12.c.3.2

The analytical model and computer code designed to predict containment pressure and temperature responses following the accidents are described in this section. A summary of the predictions is listed in Tables 6.2.1-6, 6.2.1-7, and 6.2.1-8 for short-term containment response for LOCAs, and Table 6.2.1-9 for the MSLB.

Table 6.2.1-6, Table 6.2.1-7, and Table 6.2.1-8 present thirty-eight separate cases for LOCA analysis for three postulated break locations. For the LOCA, the limiting containment pressure results from the double-ended guillotine break in the RCS hot leg piping, with the worst single failure being the loss of one ESF train.

Table 6.2.1-9 lists twenty cases for the MSLB, with four break sizes ranging from the double-ended guillotine break to the 0.5 square foot break area, and power levels from 100 percent down to zero percent of rated thermal power (RTP). The peak containment pressure results from the assumed double-ended guillotine MSLB with a failure of one MSIV at 50 percent RTP.

06.02.01-12.c.3.2

The passive heat sinks inside the primary containment consist of all painted and unpainted concrete, steel structures and liner for the containment shell and IRWST surfaces. The IRWST heat sinks are exposed to the water in the pool. The remaining heat sinks are exposed to the containment atmosphere. These areas are approximately the same temperature as the containment ambient temperature during normal plant operation. ~~The specific passive heat sinks considered in the containment pressure-temperature analysis~~The complete list of passive heat sinks in the U.S. EPR Containment and their parameters are listed in Table 6.2.1-5—Containment Heat Sink Inventory. ~~A minimum heat sink surface area was considered~~Selected heat sinks were not included in the contain ment pressure-temperature analysis for conservatism. The minimum heat sink surface area for U.S. EPR FSAR Tier 1, Section 2.1.1.1 is 64,998 m^2 or 699,633 ft^2.

The requirements of 10 CFR 50, Appendix K, Part I.A list the required features of the evaluation models for sources of heat during the LOCA. For the heat sources of 10 CFR 50, Appendix K, it must be assumed that the reactor has been operating continuously at a power level at least 1.02 times rated thermal power to allow for instrumentation error. The assumed power level may be decreased provided the proposed alternative value has been demonstrated to account for uncertainties of power level with a lower instrumentation error. The core power is measured using a secondary side heat balance with feedwater flow rate. A heat balance measurement uncertainty of approximately one-half percent of rated thermal power, or 1.005, is applicable to the core power for the U.S. EPR. This value is achieved with the use of an ultrasonic flow meter for the feedwater flow rate. This value is consistent with the assumption used in the safety analysis in Section 15.0.0.3.1.

The heat removal due to safety injection system/residual heat removal (SIS/RHR) system operation is simulated in the GOTHIC Version 7.2 computer code by specifying predicts that the containment vapor temperature remains above the design temperature for less than two minutes.

6.2.1.5 Minimum Containment Pressure Analysis for Performance Capability Studies on Emergency Core Cooling System

6.2.1.5.1 Mass and Energy Release Data

06.02.01.05-1.e

Containment pressure calculations are performed by the ICECON module within S-RELAP5 code. ICECON is a variant to the CONTEMPT containment code series. The RLBLOCA methodology treats containment pressure as a statistically varied parameter with a random sampling of the containment volume. The tabular mass and energy release data are not explicitly generated because they are part of the internal code calculations at each time step. The mathematical models that calculate the mass and energy releases to the containment are described in Section 15.6 and conform to the realistic ECCS evaluation models of ~~10 CFR 50, Appendix K~~10 CFR 50.46(a)(1)(i).

6.2.1.5.2 Initial Containment Internal Conditions

06.02.01.05-1.b

The initial values for the containment conditions are representative of 100 percent rated thermal power, and are a pressure of 14.7 psia and temperature of 59°F. The outside atmospheric temperature of 20°F and relative humidity of 100 percent are assumed and modeled within the ICECON module, which also assumes an outside atmospheric temperature of 20°F and a relative humidity of 100 percent. Inside the containment, the IRWST water temperature is expected to be at the containment temperature of ~~approximately 60~~59°F, but could range as high as 122°F, which is the Technical Specification maximum value for IRWST temperature. The RLBLOCA methodology uses the value of 122°F.

6.2.1.5.3 Other Parameters

The containment pressure varies and the RLBLOCA methodology determines it by sampling the containment volume. The nominal or best-estimate value of the containment volume is 2.888×10^6 ft^3. The upper estimate value for the containment volume is 3.645×10^6 ft^3 and represents the empty volume of the containment dome and cylinder and also neglects the volume displaced by the internal walls and structures. This latter value is conservative because a lower containment backpressure results in the highest calculated peak cladding temperature.

Heat transfer between the IRWST water and containment vapor is treated in a conservative manner. First, the IRWST is assumed to be well mixed so the liquid temperature at the interface between the IRWST water and the containment vapor space is the bulk liquid temperature. This neglects heating of the surface water and maximizes the temperature differential for heat transfer. Second, structures that reduce the exposed surface of the IRWST are neglected. Other simplifications are

Table 6.2.1-5—Containment Heat Sink Inventory
Sheet 1 of 22

06.02.01-12.c.3.2

	Description	Thickness, m					Total Surface, m^2
		Paint	C-Steel	S-Steel	Air	Concrete	
	Containment Wall with Steel Liner	0.0002	0	0.006	0.003	1.222	9177
1	Access to RB annulus	0.0002	0	0.006	0.003	1.306	77.56
2	Lower annulus rooms L1 & 2 to RB annulus	0.0002	0	0.006	0.003	1.306	151.24
3	Lower annulus rooms L3 & 4 to RB annulus	0.0002	0	0.006	0.003	1.306	151.24
4	Hot piping to RB annulus	0.0002	0	0.006	0.003	1.306	178.38
5	Middle annulus rooms L1 & 2 to RB annulus	0.0002	0	0.006	0.003	1.306	1140.81
6	Middle annulus rooms L3 & 4 to RB annulus	0.0002	0	0.006	0.003	1.3055	1269.38
7	Access to RB annulus	0.0002	0	0.006	0.003	1.306	65.95
8	Middle annulus rooms L3 & 4 to RB annulus	0.0002	0	0.006	0.003	1.306	130.42
9	Lower & upper dome L1, 2, 3 & 4 to RB annulus	0.0002	0	0.006	0.003	1.306	517.31
10	Upper annulus rooms L1 & 2 to RB annulus	0.0002	0	0.006	0.003	1.306	330.64
11	Upper annulus rooms L3 & 4 to RB annulus	0.0002	0	0.006	0.003	1.306	330.64
12	Staircase (south) to RB annulus	0.0002	0	0.006	0.003	1.306	43.7
13	Lower & upper dome L1, 2, 3 & 4 to RB annulus	0.0002	0	0.006	0.003	1.3	2309.5
14	Lower & upper dome L1, 2, 3 & 4 to RB annulus	0.0002	0	0.006	0.003	1	2480
	IRWST Vertical Wall (in contact with IRWST)	0	0	0.004	0	1.404	669
1	Spreading rooms to IRWST	0	0	0.004	0	1.2	42.06
2	IRWST to SG blowdown (LCQ) HX etc.	0	0	0.004	0	0.3	19.66
3	IRWST to components	0	0	0.004	0	0.8	37.96
4	IRWST to elevator	0	0	0.004	0	0.74	2.08
5	IRWST to lower annulus rooms L1 & 2	0	0	0.004	0	1.5	560

Table 6.2.1-5—Containment Heat Sink Inventory
Sheet 2 of 22

06.02.01-12.c.3.2

	Description	Thickness, m					Total Surface, m^2
		Paint	C-Steel	S-Steel	Air	Concrete	
6	IRWST to hot piping	0	0	0.004	0	1.5	6.88
	IRWST Vertical Wall (to Containment Atmosphere)	0.0004	0	0	0	1.404	669
1	Spreading rooms to IRWST	0.0004	0	0	0	1.2	42.06
2	IRWST to SG blowdown (LCQ) HX etc.	0.0004	0	0	0	0.3	19.66
3	IRWST to components	0.0004	0	0	0	0.8	37.96
4	IRWST to elevator	0.0004	0	0	0	0.74	2.08
5	IRWST to lower annulus rooms L1 & L2	0.0004	0	0	0	1.5	560
6	IRWST to hot piping	0.0004	0	0	0	1.5	6.88
	IRWST horizontal wall (~~floor/ceiling~~Heavy Floor)	~~0~~0.001	0	~~0.004~~0	0	1.434	547
1	IRWST to SG blowdown (LCQ) HX etc.	~~0~~0.001	0	~~0.004~~0	0	1	64.64
2	IRWST to components	~~0~~0.001	0	~~0.004~~0	0	0.8	46.56
3	IRWST to lower equipment rooms L1	~~0~~0.001	0	~~0.004~~0	0	1.5	78.8
4	IRWST to lower equipment rooms L2	~~0~~0.001	0	~~0.004~~0	0	1.5	139.2
5	IRWST to lower equipment rooms L3	~~0~~0.001	0	~~0.004~~0	0	1.5	139.2
6	IRWST to lower equipment rooms L4	~~0~~0.001	0	~~0.004~~0	0	1.5	78.8
	IRWST Horizontal Wall (IRWST Ceiling)	0	0	0.004	0	1.5	436
1	IRWST to lower equipment rooms L1	0	0	0.004	0	1.5	78.8
2	IRWST to lower equipment rooms L2	0	0	0.004	0	1.5	139.2
3	IRWST to lower equipment rooms L3	0	0	0.004	0	1.5	139.2
4	IRWST to lower equipment rooms L4	0	0	0.004	0	1.5	78.8
	IRWST Basemat	0	0	0.004	0	4	590

Table 6.2.1-5—Containment Heat Sink Inventory
Sheet 3 of 22

06.02.01-12.c.3.2

	Description	Thickness, m Paint	C-Steel	S-Steel	Air	Concrete	Total Surface, m^2
1	IRWST to ground	0	0	0.004	0	4	590
	Building Basemat (Excluding IRWST)	0.001	0	0	0	4.0	720
1	Spreading rooms to ground	0.001	0	0	0	4.0	175
2	Access area to ground	0.001	0	0	0	4.0	80
3	SIS pipe penetrations to ground (To SB 1&2)	0.001	0	0	0	4.0	144
4	SIS pipe penetrations to ground (To SB 3&4)	0.001	0	0	0	4.0	142
5	Fuel Building penetrations to ground	0.001	0	0	0	4.0	172
6	Elevator shaft penetrations to ground	0.001	0	0	0	4.0	6.72
	Vertical wall to accessible space	0.0004	0	0	0	0.39	8342
1	access to elevator	0.0004	0	0	0	0.1	52.34
2	lower annulus rooms L1 & 2 to elevator	0.0004	0	0	0	0.1	12.54
3	lower annulus rooms L1 & 2 to access	0.0004	0	0	0	0.1	14.08
4	lower annulus rooms L3 & 4 to access	0.0004	0	0	0	0.1	27.56
5	lower annulus rooms L1 & 2 to hot piping	0.0004	0	0	0	0.15	20.8
6	lower annulus rooms L3 & 4 to hot piping	0.0004	0	0	0	0.15	20.8
7	middle annulus rooms L1 & 2 to staircase (south)	0.0004	0	0	0	0.15	362.82
8	middle annulus rooms L1 & 2 to elevator	0.0004	0	0	0	0.1	178.94
9	Internal wall in middle annulus rooms L1 & 2	0.0004	0	0	0	0.1322	186.96
10	Internal wall in middle annulus rooms L1 & 2	0.0004	0	0	0	0.25	190.24
11	middle annulus rooms L1 & 2 to access	0.0004	0	0	0	0.1	17.8
12	middle annulus rooms L3 & 4 to access	0.0004	0	0	0	0.1	16.38
13	Internal wall in middle annulus rooms L3 & 4	0.0004	0	0	0	0.25	203.96

Table 6.2.1-5—Containment Heat Sink Inventory
Sheet 22 of 22

	Description	Thickness, m Paint	C-Steel	S-Steel	Air	Concrete	Total Surface, m^2
14	Internal steel in surge line, below	0.0002	0.0015	0	0	0	109.56
15	Internal steel in middle equipment rooms L3	0.0002	0.0015	0	0	0	454.34
16	Internal steel in middle equipment rooms L4	0.0002	0.0015	0	0	0	427.97
17	Internal steel in middle equipment rooms L1	0.0002	0.0015	0	0	0	428.09
18	Internal steel in middle equipment rooms L2	0.0002	0.0015	0	0	0	454.31
19	Internal steel in PZR	0.0002	0.0015	0	0	0	16.03
20	Internal steel in upper equipment rooms L3 & 4	0.0002	0.0015	0	0	0	415.34
21	Internal steel in upper equipment rooms L1 & 2	0.0002	0.0015	0	0	0	415.34
22	Internal steel in upper annulus rooms L3 & 4	0.0002	0.0015	0	0	0	54.4
23	Internal steel in lower & upper dome L1, 2, 3 & 4	0.0002	0.0015	0	0	0	1392.85
24	Internal steel in upper annulus rooms L1 & 2	0.0002	0.0015	0	0	0	77.6
25	Internal steel in staircase (south)	0.0002	0.0015	0	0	0	5.8
				Cumulative Available Surface Area			67,646 (728,136 ft^2)
				Minimum Surface Area			64,998 (699,633 ft^2)

06.02.01-12.c.3.2

06.02.01.02-1.a.2

Table 6.2.1-10—Critical Subcompartments in Containment

Room Name (30UJA)	Room Description	System Name (Pipe Name)	Operating Pressure (psia)	Operating Temperature (°F)	NPS (in)	Accident Pressure (psia)
11 - 004	SG Loop 2	SIS/RHR (J~~NG23 BR002~~JNA20 BR001)	~~710.7~~2250.0	~~77.0~~625.7	~~12~~10	~~*~~20.80
11 - 006	RCP Loop 3	CVCS (KBA35 BR002)	2324.0	512.3	4	*
11 - 027	SI valves Loop 3	SIS/RHR (JNG33 BR001)	~~710.7~~814.7	~~77.0~~140	12	~~*~~16.90
15 - 004	SG Loop 2	CVCS (KBA34 BR019)	2324.0	512.3	3	*
15 - 006	RCP Loop 3	SIS/RHR(JNG33 BR007)	2250.0	563.4	10	29.02
18 - 004	SG Loop 2	SG Blowdown (LCQ10 BR012)	1144.3	561.0	2	*
23 - 004	SG Loop 2	FW(LAB70 BR005)	1131.2	446.3	20	28.36
29 - 004	SG Loop 2	FW(LAB70 BR005)	1131.2	446.3	20	31.07
29 - 019	Pressurizer Cavity	RCS (JEF10 BR004)	2250.0	653.0	6	17.82
34 - 004	SG Loop 2	SG (JEA20 BR302)	1123.0	559.0	1	*
34 - 019	Pressurizer Relief Valve Cavity	RCS (JEF10 BR004)	2250.0	653.0	6	18.59

06.02.01.02-1.a.2

Table 6.2.1-15—High Energy Lines in Critical Subcompartments

Room Name (30 UJA)	Pipe Name	Pressure (psia)	Temp. (°F)	Pipe ID (in)	Enthalpy (BTU/lb_m)	Mass Flux (lb_m/ft^2- s)	CSA (ft^2)	Energy Flux (MMBTU/hr)
11 - 004	~~JNG23 BR002~~JNA20 BR001	~~710.7~~2250	~~77.0~~625.7	~~10.126~~8.5	~~47.0184~~651.8	~~12243.9100~~15831.9	~~0.5592~~0.394	~~2.3180564~~14.638101 x10^3
11 - 006	KBA35 BR002	2324.0	512.3	3.438	501.7042	16233.5300	0.0645	3.7803532x10^3
11 - 027	JNG33 BR001	~~710.7~~814.7	~~77.0~~140.0	~~11.750~~11.376	~~47.0184~~110.0	~~12243.9100~~22292.1	~~0.7530~~0.706	~~3.1212164~~12.4618588x10^3
15 - 004	KBA34 BR019	2324.0	512.3	2.624	501.7042	16233.5300	0.0376	2.2021571x10^3
15 - 006	JNG33 BR007	2250.0	563.4	8.500	See Table 6.2.1-16			
18 - 004	LCQ10 BR012	1144.3	561.0	1.687	563.5935	3657.1790	0.0155	2.303574x10^2
23 - 004	LAB70 BR005	1131.2	446.3	17.000	See Table 6.2.1-17			
29 - 004	LAB70 BR005	1131.2	446.3	17.000	See Table 6.2.1-17			
29 - 019	JEF10 BR004	2250.0	653.0	5.187	1116.8417	2968.1370	0.1467	3.5024176x10^3
34 - 004	JEA20 BR302	1123.0	559.0	0.815	1187.7103	1384.4530	0.0036	4.28908x10^1
34 - 019	JEF10 BR004	2250.0	653.0	5.187	1116.8417	2968.1370	0.1467	3.5024176x10^3